

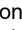

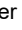

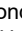
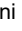
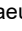


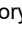



RESEARCH ARTICLE | MAY 04 2023

Perspective: Nanophotonic electro-optics enabling THz bandwidths, exceptional modulation and energy efficiencies, and compact device footprints

Larry R. Dalton ; Juerg Leuthold ; Bruce H. Robinson ; Christian Haffner ; Delwin L. Elder ; Lewis E. Johnson ; Scott R. Hammond ; Wolfgang Heni ; Claudia Hosessbacher; Benedikt Baeuerle ; Eva De Leo ; Ueli Koch ; Patrick Habegger; Yuriy Fedoryshyn ; David Moor; Ping Ma 



APL Mater 11, 050901 (2023)
<https://doi.org/10.1063/5.0145212>




View Online



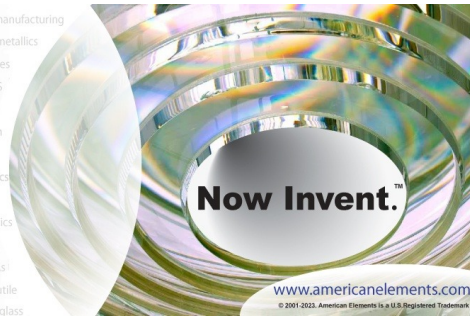
Export Citation

CrossMark



yttrium iron garnet glassy carbon beamsplitters fused quartz additive manufacturing
 zeolites III-IV semiconductors gallium lump copper nanoparticles organometallics
 nano ribbons barium fluoride europium phosphors photonics infrared dyes
 sapphire windows Nd:YAG epitaxial crystal growth ultra high purity materials transparent ceramics CIGS
 spintronics raman substrates cerium oxide polishing powder cermet nanodispersions
 silver nanoparticles perovskites surface functionalized nanoparticles MBE grade materials thin film
 MOCVD beta-barium borate OLED lighting solar energy
 rare earth metals quantum dots sputtering targets fiber optics
 osmium scintillation Ce:YAG h-BN deposition slugs
 refractory metals laser crystals CVD precursors photovoltaics
 anodic aluminum oxide niobate InAs wafers metamaterials borosilicate glass
 ZnS CdTe MOFs AuNPs YBCO superconductors InGaAs
 perovskite crystals transparent ceramics indium tin oxide MgF2 rutile optical glass
 diamond micropowder

The Next Generation of Material Science Catalogs



Now Invent.™

www.americanelements.com
 © 2001-2022, American Elements LLC, a U.S. Registered Trademark

Perspective: Nanophotonic electro-optics enabling THz bandwidths, exceptional modulation and energy efficiencies, and compact device footprints

Cite as: APL Mater. 11, 050901 (2023); doi: 10.1063/5.0145212

Submitted: 3 February 2023 • Accepted: 23 March 2023 •

Published Online: 4 May 2023



View Online



Export Citation



CrossMark

Larry R. Dalton,^{1,a)} Juerg Leuthold,² Bruce H. Robinson,¹ Christian Haffner,³ Delwin L. Elder,^{1,4} Lewis E. Johnson,^{1,4} Scott R. Hammond,^{1,4} Wolfgang Heni,⁵ Claudia Hosessbacher,⁵ Benedikt Baeuerle,⁵ Eva De Leo,⁵ Ueli Koch,² Patrick Habegger,⁵ Yuriy Fedoryshyn,² David Moor,² and Ping Ma²

AFFILIATIONS

¹ University of Washington, Departments of Chemistry and Electrical Engineering, Seattle, Washington 98195-1700, USA

² ETH Zurich, Institute of Electromagnetic Fields (IEF), 8902 Zurich, Switzerland

³ IMEC, Remisebosweg 1, 3001 Leuven, Belgium

⁴ NLM Photonics, Seattle, Washington 98195, USA

⁵ Polariton Technologies AG, 8803 Ruschikon, Switzerland

^{a)} Author to whom correspondence should be addressed: dalton@chem.washington.edu

ABSTRACT

The growth of integrated photonics has driven the need for efficient, high-bandwidth electrical-to-optical (EO) signal conversion over a broad range of frequencies (MHz–THz), together with efficient, high bandwidth photodetection. Efficient signal conversion is needed for applications including fiber/wireless telecom, data centers, sensing/imaging, metrology/spectroscopy, autonomous vehicle platforms, etc., as well as cryogenic supercomputing/quantum computing. Diverse applications require the ability to function over a wide range of environmental conditions (e.g., temperatures from <4 to >400 K). Active photonic device footprints are being scaled toward nanoscopic dimensions for size compatibility with electronic elements. Nanophotonic devices increase optical and RF field confinement via small feature sizes, increasing field intensities by many orders of magnitude, enabling high-performance Pockels effect materials to be ultimately utilized to their maximum potential (e.g., in-device voltage-length performance ≤ 0.005 V mm). Organic materials have recently exhibited significant improvements in performance driven by theory-guided design, with realized macroscopic electro-optic activity (r_{33}) exceeding 1000 pm/V at telecom wavelengths. Hybrid organic/semiconductor nanophotonic integration has propelled the development of new organic synthesis, processing, and design methodologies to capture this high performance and has improved understanding of the spatial distribution of the order of poled materials under confinement and the effects of metal/semiconductor-organic interfaces on device performance. Covalent coupling, whether from *in situ* crosslinking or sequential synthesis, also provides a thermally and photochemically stable alternative to thermoplastic EO polymers. The alternative processing techniques will reduce the attenuation of r_{33} values observed in silicon organic hybrid and plasmonic organic hybrid devices arising from chromophore-electrode electrostatic interactions and material conductance at poling temperatures. The focus of this perspective is on materials, with an emphasis on the need to consider the interrelationship between hybrid device architectures and materials.

© 2023 Author(s). All article content, except where otherwise noted, is licensed under a Creative Commons Attribution (CC BY) license (<http://creativecommons.org/licenses/by/4.0/>). <https://doi.org/10.1063/5.0145212>

INTRODUCTION

For more than a decade, international technology market demands and governmental/professional society studies have emphasized^{1–5} that chip-scale integration of photonics and electronics is critical for next generation information technology.^{6,7} The size disparity between photonic and electronic circuits has historically inhibited the realization of this goal. Recently, the advent of nanophotonic technologies (silicon photonics, plasmonics, meta-surface devices, etc.) has facilitated photonic/electronic circuit integration and resulted in dramatic improvements in bandwidth, modulation efficiency (voltage-length performance, $V_{\pi}L$), and energy efficiency for information technology applications.^{7,8} This transition to nanophotonic architectures has the highest impact for devices relying on the Pockels effect. Device lengths have been reduced from centimeters to micrometers while maintaining CMOS level drive voltages.^{7,9} The transformative improvement in voltage-length performance (as much as a factor of 10 000) stems from two effects: (1) concentration and improved overlap of low frequency (radio frequency/microwave/millimeter wave) fields and telecommunication wavelength (1.3 and 1.55 μm) optical fields between nanoscale electrode separations; and (2) theory-guided improvement of in-device electro-optic (EO) activity of organic materials, which can deliver a particularly high Pockels response.^{7,9}

However, the transition from mesoscale to nanoscale dimensions substantially changes design considerations for such high-performance organic materials, including requiring close coordination between the design of materials and device architectures. Interfacial interactions between EO materials and device drive electrodes become highly significant in the smallest devices with the highest optical mode confinement.^{7,10,11} The reduction of electrode separation to nanoscopic dimensions has made sequential synthesis processing, in which materials are quasi-deterministically grown from a surface, viable. This is due to the much smaller number of layers required compared to the number required for mesoscopic devices. Covalent coupling/sequential synthesis permits the avoidance of attenuation of EO activity in the vicinity of electrodes and avoids the problem of attenuation of poling-induced EO activity due to conductance effects [eliminating the need for charge blocking layers between electrodes and organic electro-optic (OEO) materials]. With conventional poling and slot waveguide architectures, acentric order is attenuated in the narrowest slots due to interfacial effects. Sequential synthesis^{6,7} has the highest order at the interface, maximizing potential performance in narrower slots and affording the best prospects for further performance improvements and production scalability in nanoscale hybrid EO devices.

There are additional benefits resulting from OEO material deposition techniques like sequential synthesis. While poling a single device is straightforward, simultaneously poling hundreds of devices per chip or thousands of devices per wafer may impose challenges to the adoption of the technology due to potentially limited production throughput and yield issues. Robotically-implemented sequential synthesis can provide a robust and reproducible OEO processing technique that is scalable from device to chip to wafer. Furthermore, since the chromophore multilayers will be attached to one another through chemical bonds, they will exhibit excellent

thermal and photochemical stability, matching or exceeding what is achievable with the best crosslinked electrically poled materials. A final advantage of sequential synthesis is that it would enable the use of chromophores with exceptional hyperpolarizabilities (β) that are not processible (or difficult to process) by electric field poling due to leakage current related concerns at poling (material glass transition) temperatures. Previously, it was found that some of the highest β chromophores had too high a leakage current to be poled at high density and could only be poled in a polymer host,¹² which dilutes the EO effect; sequential synthesis alleviates these concerns. However, electric field poling will continue to be the processing protocol of choice for certain device architectures and applications. However, nanophotonics has facilitated an important expansion of processing options.

Integration of EO materials into nanophotonic device architectures has also forced a change in perspective with respect to the consideration of material propagation loss. The propagation loss of active EO materials becomes important only when that loss approaches the propagation loss of passive photonic/plasmonic circuit elements (silicon photonic, plasmonic, and meta-surface elements). Compact device architectures with short interaction (propagation) lengths lead to low total insertion loss.^{7,8}

While photonic integration was initially driven by telecom and datacom applications, the application space has increased dramatically with emerging applications related to sensors, displays, and metrology, e.g., LIDAR and autonomous vehicles, which are of growing importance for environmental monitoring, agriculture, archeology, transportation, and defense.

To understand the optimization of electro-optic devices, a brief review of the fundamental symmetry requirement of second-order nonlinear optical (NLO) activity is necessary. Second order NLO activity (EO modulation, optical rectification, second harmonic generation, sum, and difference frequency generation) of organic materials requires that fundamental molecular units (chromophores) exhibit not only molecular asymmetry (dipolar, noncentrosymmetric, or acentric symmetry), but also that the supramolecular organization of these chromophores is acentric.^{6,13} For such materials, acentric organization is accomplished by crystal growth (under special conditions), self-assembly/sequential synthesis, or electric field poling.^{6,7} For photonics applications, ordering via electric field poling has proven to be the only viable option for mesoscopic OEO materials.^{6,7,14} Crystal growth has been found to be impossible for organic chromophores with the largest molecular first hyperpolarizabilities, and too many sequential synthesis steps are required for mesoscale materials.^{6,7} Guidance from multi-scale modeling has permitted dramatic improvements in both molecular first hyperpolarizabilities via the use of quantum mechanical calculations^{7–9,12,15–17} and electric field poling induced acentric chromophore organization via statistical mechanical methods.^{7,18–20} With respect to electro-optics, mesoscale device architectures inhibited Pockels effect materials from significantly exceeding the performance of nanoscale electro-absorptive (EA) devices, even though devices based on EA materials¹ suffer from high optical loss (absorption), limited bandwidth (due to excited state lifetimes), and poor signal linearity (signal distortion due to simultaneous changes in absorbance and index of refraction called “chirp”).

The converse of electrical-to-optical signal transduction (electro-optics) is optical-to-electrical signal transduction (optical

rectification), which is another aspect of second order optical non-linearity. Mesoscale optical rectification devices are even more disadvantageous relative to conventional inorganic photodetector devices based on electron excitation (absorption) followed by free carrier generation. This is the case even though optical rectification does not involve electron excitation to excited states and thus enables lower optical loss—“Transparent photodetection,” which has a lower noise floor and a larger bandwidth.^{7,9,21–23}

The performance of second-order NLO materials has been dramatically improved with integration into nanophotonic device architectures, which has been key to chip-scale integration of electronics and photonics as well as improving the size, weight, power, cost, and performance (SWaP-CP) of devices and systems. The concentration of radio frequency/microwave/millimeter wave, and telecommunication [1.3 μm (O band) to 1.55 μm (C band) wavelength] optical fields in devices of nanoscale dimensions dramatically enhances effective optical nonlinearity.⁷ Such field concentration occurs in silicon photonic,^{5,7,24–63} plasmonic,^{7,8,10,15,61–98} and plasmonic meta-surface devices.^{7,99–115} All of these emerging technologies are critical to the chip-scale integration of electronics and photonics.^{7,90} Component-level improvement in performance (e.g., $V_{\pi}L$) as a function of reducing device dimensions is illustrated for hybrid devices in Fig. 1.⁷ The use of thin film lithium niobate (TFLN) in silicon photonic device architectures permits modulation efficiencies as low as ~50 V·mm. Incorporation of third generation OEO materials in plasmonic organic hybrid (POH) devices delivers large improvements in both RF/optical mode confinement and overlap and the enhanced Pockels effect from high performance OEO materials. The slow light effect⁶⁵ can also contribute, becoming dominant in plasmonic devices (relative to silicon photonic devices) for slot widths of 20–30 nm. POH devices

afford low RC time constants and THz bandwidths. Energy efficiency on the order of 10 s of attoJoules(aJ)/bit is possible.^{7,95} The electrical power consumption of a device scales with capacitance and voltage as $C V^2$. Photonic devices can be made longer than plasmonic devices while maintaining acceptable insertion loss, enabling lower drive voltages, and providing another route to lower power use. Exploiting the full potential of current >1000 pm/V mesoscopic OEO materials in even narrower waveguides would enable modulation efficiencies below 0.005 V·mm, critical for achieving energy efficiencies <10 aJ/bit and sub-μm² device footprints as well as THz bandwidths. These schemes represent an important material design paradigm shift necessitated by nanophotonic architectures.^{7,8}

However, it should be kept in mind that the hybrid integration of Pockels effect materials (OEO, lithium niobate, or barium titanate) with silicon and/or silicon nitride photonics is a highly competitive technology that enables lower optical loss.^{7,24–47,49–52,59,60,116,117} Different applications have different requirements for modulation efficiency (voltage-length performance, $V_{\pi}L$), bandwidth, energy efficiency, optical insertion loss, and device footprint, and thus no single material/device technology is ideal for all applications. In like manner, a given material processing protocol, such as electric field poling or sequential synthesis, may be preferred for one device architecture but not another. Obviously, crystal growth is an important processing methodology for inorganic materials. Control of optical signals can also be accomplished using thermos-optic and MEMS devices and phase-change materials; however, such devices typically have much lower bandwidths (Hz–MHz) and will not be discussed here.

The $V_{\pi}L$ for various device architectures and the relationship to a material’s Pockels effect response are graphically depicted in Fig. 2,

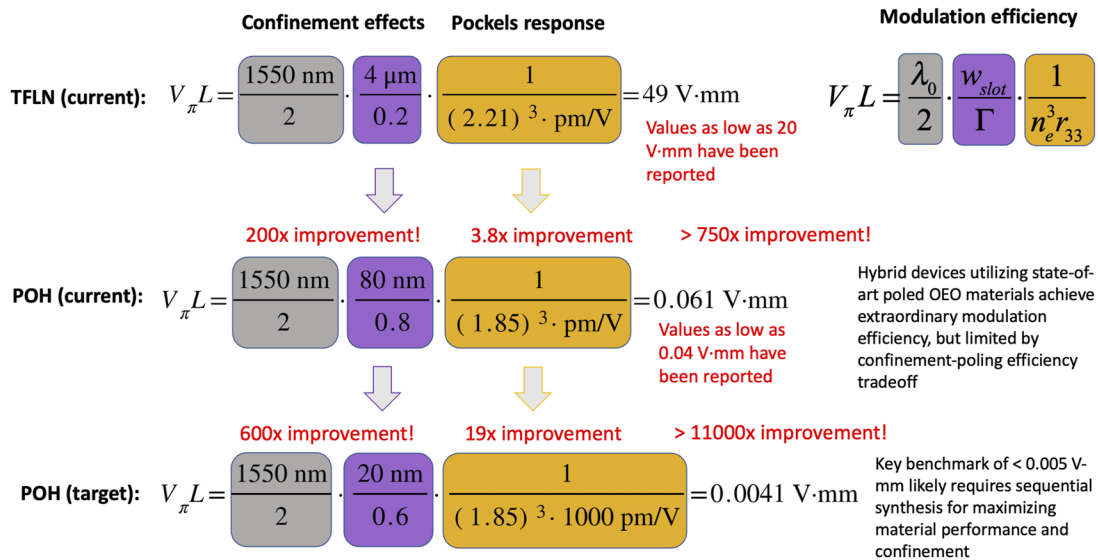


FIG. 1. Comparison of $V_{\pi}L$ values in current thin film lithium niobate (TFLN), current plasmonic organic hybrid (POH), and anticipated future POH technology. λ_0 is the wavelength of the optical signal, w_{slot} is the device slot width (and electrode separation distance), Γ is the overlap factor of the RF field and optical mode, n_e is the extraordinary index of refraction of the EO material, and r_{33} is the EO coefficient.

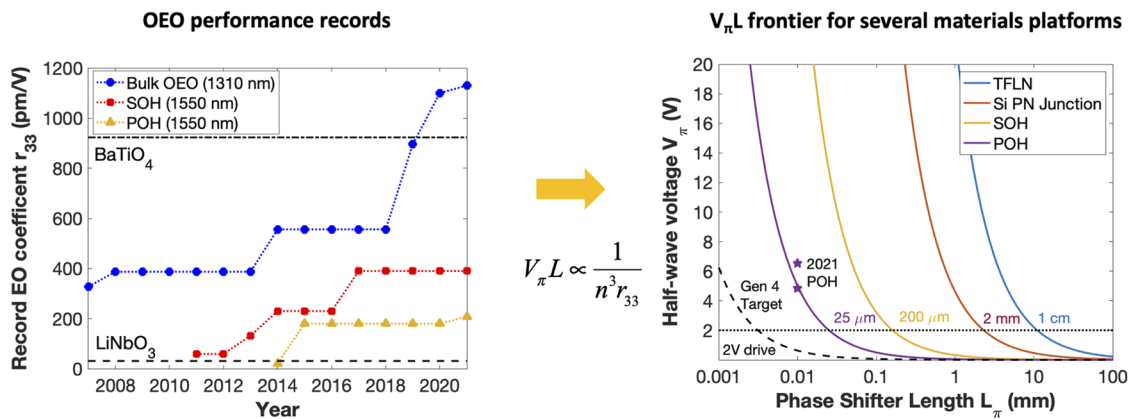


FIG. 2. Left: The improvement of EO activity with time is shown for various EO materials and device architectures. In-device performance has lagged bulk material performance by several years due to the process optimization required for effective implementation in nanophotonic devices, including addressing the problem of attenuation of EO activity due to electrode–chromophore electrostatic interactions and material conductance at poling temperatures. Covalent modification of electrode surfaces (e.g., as in sequential synthesis) is a means of mitigating the reductions in r_{33} seen with SOH and POH devices (left). Right: Calculated modulation efficiency (voltage-length performance) is illustrated for lithium niobate, silicon PN junction devices, silicon-organic hybrid (SOH) devices, and plasmonic-organic hybrid (POH) devices.⁷ It is important to keep in mind that while $V_{\pi}L$ is an important metric, it is not the only metric relevant for optimizing device performance.⁷

right. Fig. 2, left, illustrates the evolution of the electro-optic activity (r_{33}) for electrically-poled organic materials with time. The reduction of r_{33} in SOH and POH devices relative to values for mesoscopic thin films is due to electrostatic interaction between chromophores and electrodes and to electric conductance through organic films at poling temperatures. As will be discussed in more detail shortly, this attenuation can be eliminated by the covalent coupling/sequential synthesis material processing schemes.

The situation is equally dramatic for optical rectification,^{7,9,21–23} permitting potential improvement in photodetection responsivity R from values orders of magnitude below inorganic photodiodes to values comparable to photodiodes at high GHz frequencies (~ 1 ampere/watt, A/W), and exceeding values for photodiodes at THz frequencies. However, photodetection technology is rapidly evolving, including with the introduction of new materials such as graphene.^{94,118–124}

Integration of second order NLO (Pockels effect) materials into nanophotonic device architectures has significant implications for device optical insertion loss (the sum of propagation and coupling loss).^{6,7} The optical propagation loss at telecommunication wavelengths associated with passive silicon photonic (~ 2 dB/mm) and plasmonic (~ 0.2 dB/ μm) waveguides is typically higher than that of lithium niobate (<0.2 dB/cm), silicon nitride (<0.2 dB/cm), and macroscopic organic materials (1–10 dB/cm).^{7,8,61,65,71} Short device dimensions are thus required—but also feasible—for hybrid silicon photonic and plasmonic devices. The propagation loss associated with active materials becomes relevant only when such losses are comparable to the optical loss of passive waveguide elements.^{7,74} Coupling losses can be comparable or even greater than propagation losses and are a challenge for nanophotonic devices, but they are being reasonably addressed.^{6,7,125,126}

Second order nonlinear optical waveguide devices (e.g., EO modulators) can be divided into three categories: (1) traveling wave and lumped element devices (e.g., phase shifters arranged

in an interferometric configuration to form an amplitude modulator);^{6–8,61,71} (2) resonant devices, such as ring resonators, that involve multiple passes of light through devices (with the number of passes quantified by the device's quality factor, Q);^{6,7} and (3) resonant antennas.^{7,69,70,78} Resonant architectures yield compact devices and improved sensitivity because of the longer effective interaction length between the optical and RF fields in the device, but this increased sensitivity comes at the expense of bandwidth (as the dwell time of interacting fields in the device is increased). Resonant devices such as ring resonators permit special applications such as wavelength division multiplexing (WDM) and comb generation (including Pockels and Kerr effect hybrid devices) to be accomplished straightforwardly and, in special configurations, can be used to achieve low insertion loss.^{7,76,77} The sensitivity of sensors can be improved using resonant devices; device energy efficiency is also improved by the Q of resonant devices (e.g., the energy efficiency of state-of-the-art simple phase modulators is on the order of 70 aJ/bit,^{7,95} but even modest Q resonant devices can yield energy efficiencies <10 aJ/bit). The fundamental building block of electro-optical signal conversion for telecommunications is the phase modulator; combining two phase modulators in an interferometer configuration yields a balanced Mach–Zehnder amplitude modulator, and combining two Mach–Zehnder modulators yields an in-phase-quadrature (IQ) modulator that permits control of both amplitude and phase for telecommunication signals, enabling higher-order modulation schemes.^{7,8,32,36,44–47,68,79,93} A final EO device architecture that is critical for telecommunication and other applications is the resonant antenna.^{7,69,70,78} In these devices, an antenna is coupled directly to an EO modulator, allowing electrical-to-optical conversion of wireless/free space signals, extending their applicability to millimeter wave wireless and satellite communications applications, and permitting the elimination of low noise amplifiers (LNAs).^{7,69,70,78} Representative recent advances are graphically highlighted in Fig. 3.

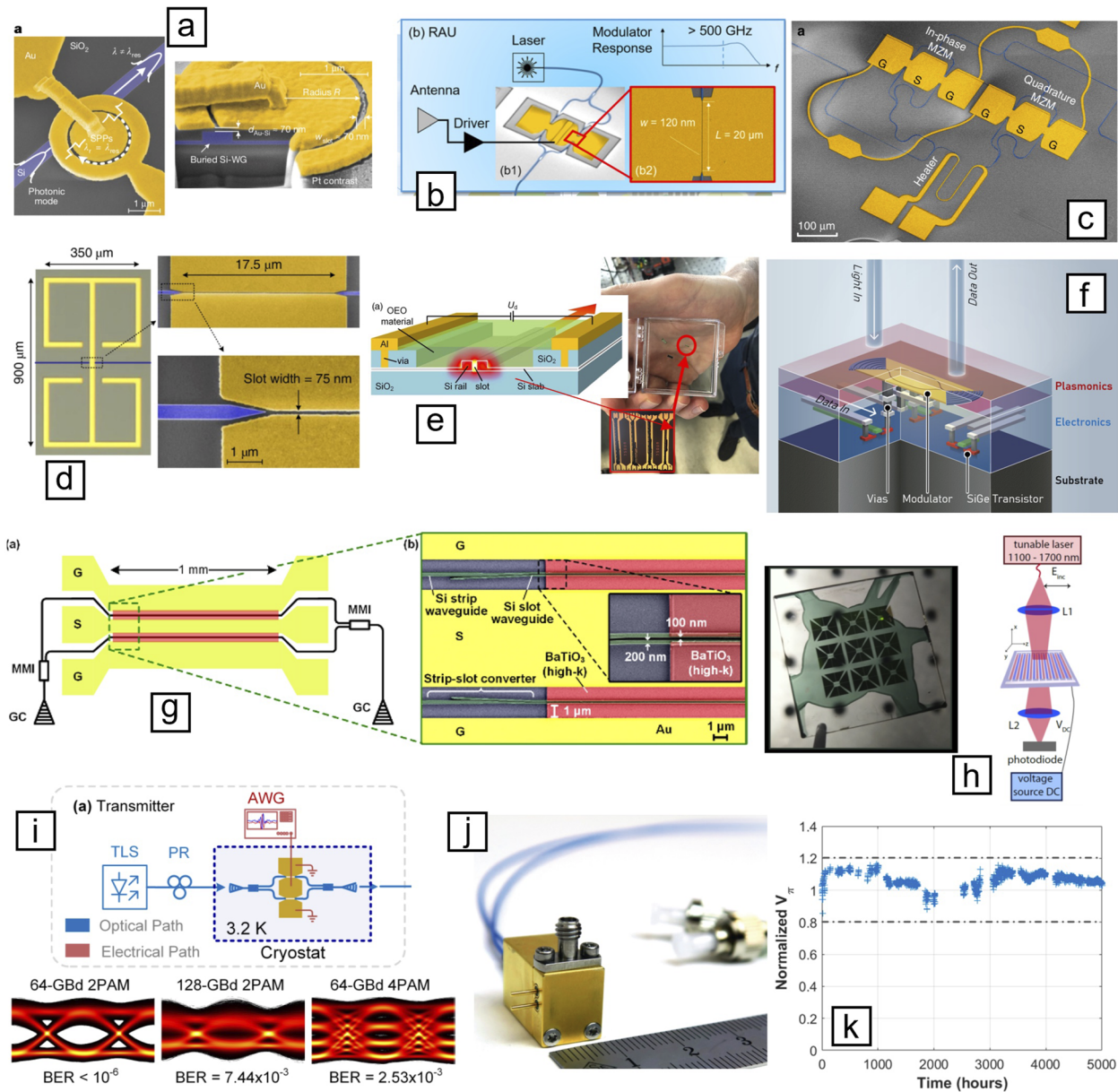


FIG. 3. Advances in OEO devices: (a) a high-efficiency ultra-compact plasmonic organic hybrid (POH) ring resonator;⁷³ (b) compact POH Mach-Zehnder modulator (MZM) demonstrating flat frequency response beyond 500 GHz, high power handling, and high linearity;⁸² (c) an ultra-efficient high speed POH in-phase-quadrature (IQ) modulator;⁹⁵ (d) a compact 60 GHz mm wave POH mixer/antenna;⁷⁸ (e) a low-voltage sub-mm SOH MZM;⁴² (f) >100 Gbit/s monolithically integrated POH-SiGe BiCMOS transmitter;⁹⁰ (g) >76 GHz capacitively coupled SOH MZM;⁵⁰ (h) an active POH meta-surface spatial light modulator operating at >50 MHz;¹⁰⁴ (i) 128 GBd 2PAM, 64 GBd 4PAM POH modulator operating at 4 K;¹²⁷ (j) a discrete POH modulator containing the HLD¹²⁶ chromophore commercialized by Polariton Technologies (<https://www.polariton.ch>); (k) an encapsulated POH modulator containing HLD showing excellent V_{π} photostability over 5000 h in air at 0 dBm 1550 nm laser power.¹²⁹

In the following, we discuss the theory-guided development of organic materials suitable for exploiting nanophotonic device architectures. We divide the discussion into three sections: (1) improvement of the first molecular hyperpolarizability of fundamental chromophore units relevant to different types of

device architectures;^{6,7,11,12,17,128,130–140} (2) improvement and retention of the acentric order of chromophores in nanophotonic devices, including consideration of interfacial effects involving chromophores and electrodes;^{6–8,10,18–20} and (3) expansion of processing options (sequential synthesis in addition to electric field poling) for

nanophotonic devices and influence on in-device material activity and material thermal/photochemical stability.^{6,7}

Optimizing molecular first hyperpolarizability under optical loss constraints.^{7,11,12,14,17,128,130–140} Initially, quantum mechanical calculations aimed at understanding and improving molecular first hyperpolarizability (β) evolved through two stages. The first focused on finding computationally efficient yet accurate computational approaches for single-molecule calculations for chromophore development and characterization. This has largely focused on developing improved density functional theory (DFT) calculations benchmarked against higher order calculations such as MP2 and coupled cluster methods, etc.^{128,130,132,137} An important aspect of this approach was understanding linear optical properties, such as absorption loss (k), as well as optical nonlinearity (including β). This undertaking has been highly successful, particularly with respect to understanding the variation of β and k with changes in chromophore structure and conformation.^{7,12,17,139} DFT calculations have also increased our understanding of the effects of the dielectric environment (permittivity) on chromophore properties.^{12,133}

A complementary effort has focused on computing the effect of intermolecular chromophore–chromophore excitonic (excitonic) interactions on properties.^{15,140} An important component of this second stage of computation was the use of chromophore ensemble information obtained from coarse-grained statistical mechanical (e.g., Monte Carlo) calculations to carry out quantum mechanical calculations on realistic chromophore distributions.⁷ An important observation of this effort was that for materials with low acentric (poling-induced) order, the effect of excitonic interactions on molecular hyperpolarizability largely averaged out,⁷ though such calculations may be needed for more highly ordered systems developed with sequential synthesis.

More recent single-molecule calculation efforts have focused on the identification of optimum β values for materials with acceptable optical loss for specific device architectures. The transition from mesoscale to nanophotonic hybrid devices has altered requirements for optical propagation loss in OEO materials; instead of being the primary contributor to optical loss, loss is constrained by the loss of the underlying passive waveguide (e.g., silicon photonic or plasmonics). To be desirable, OEO materials should not substantially increase that loss unless they also yield an improvement in modulation efficiency that is substantially more than the insertion loss penalty, a trade-off already experienced in silicon vs plasmonic platforms. This change in design requirements, combined with an improved understanding of reliable methods for predicting chromophore optical properties using density functional theory,^{12,15,136,142} enabled a search for chromophores with higher hyperpolarizabilities and propagation losses that would not have been acceptable for mesoscale devices.^{12,16,17} In general, hyperpolarizability increases with smaller band gaps, with the typical relation given by the two-level model.^{131,143} Searches have been performed under the constraints of ground-state dipole moments and shape similarity with existing high-performance chromophores. These searches demonstrated that substantial headroom still exists for improving hyperpolarizability, as previously suggested by theory,^{20,131,135} and have led to chromophores with greatly enhanced hyperpolarizability in solution based on stronger electron donating moieties.^{7,12,17} However, further optimization was

required to translate to material-level performance due to the high dielectric sensitivity of chromophore optical properties and excessive optical loss. Gradual reduction of donor strength permitted the realization of high material performance with lower loss by shifting the chromophores further from the cyanine limit (where the HOMO and LUMO are essentially degenerate in energy and the bandgap is thus extremely small); contributions of multiple electron-donating moieties of different strengths may also play a role in obtaining high hyperpolarizability without excessive absorption due to an excessively red-shifted primary charge transfer band.¹⁷ Constraints are more acute for O-band systems (1.3 μm), where the operating wavelength is closer to the principal charge transfer band edge, and for quantum information science systems on low-loss photonics platforms. This has led to applying similar techniques to those that have been used for improving hyperpolarizability for reducing optical loss at the cost of some EO response while minimizing that reduction in response to maximizing r_{33}/k , where r_{33} is the EO coefficient and k is absorption loss. If ultra-high bandwidth is not required, in some cases, a longer device may still permit lower total insertion loss on platforms with less lossy passive components.

Understanding and optimizing chromophore ordering considering intermolecular interactions including understanding and mitigating interfacial interaction effects.^{6–8,10,18–20,144} Fully atomistic molecular dynamics (MD) methods are extensively used to simulate the behavior of molecular ensembles.^{7,145–147} However, the slow timescale of poling-induced alignment vs local dynamics has limited the applicability of conventional MD to OEO materials to date.^{15,18,20} The essential interactions for the organization of electrically-poled chromophores include chromophore-poling field interactions and spatially anisotropic electrostatic and non-electrostatic chromophore–chromophore interactions, including the rearrangement of flexible side chains. Coarse-graining of chromophores via the Level-of-Detail (LoD) method,^{7,18–20} together with enhancing the rate of convergence of simulations via the Adiabatic Volume Adjustment (AVA) method,^{18,20,148} has permitted efficient simulation of the effect of these interactions and identification of the effect of chromophore shape and charge distribution on material EO activity. Ensemble organization from these coarse-grained calculations can in turn be mapped back to fully atomistic models to investigate the effect of chromophore–chromophore excitonic interactions using quantum mechanical methods.^{15,138,140} Simulations of poling-induced acentric order (and hence EO activity and index of refraction properties) exploiting the LoD and AVA methods have led to efficient and accurate simulations of the dependence of properties on chromophore structure.^{7,20}

Driven by the observation of reduced EO activity in narrower slot waveguides, theoretical and computational methods have also been used to investigate the effect of interfacial interactions between chromophores and poling electrodes (see Fig. 4).^{7,8,10,11,15,144} Simulation results showed a fall-off in ordering due to dipole-induced/dipole interactions between the chromophores and the (gold or doped semiconductor) walls of the slot waveguide (electrodes), consistent with experiment and with a scaled freely rotating dipole-based theoretical model.^{11,17,144}

Simulations of the centric order parameter, $\langle P_2 \rangle$, in POH devices show that this attenuation is associated with chromophores lying parallel to the electrode surfaces (orthogonal to the poling

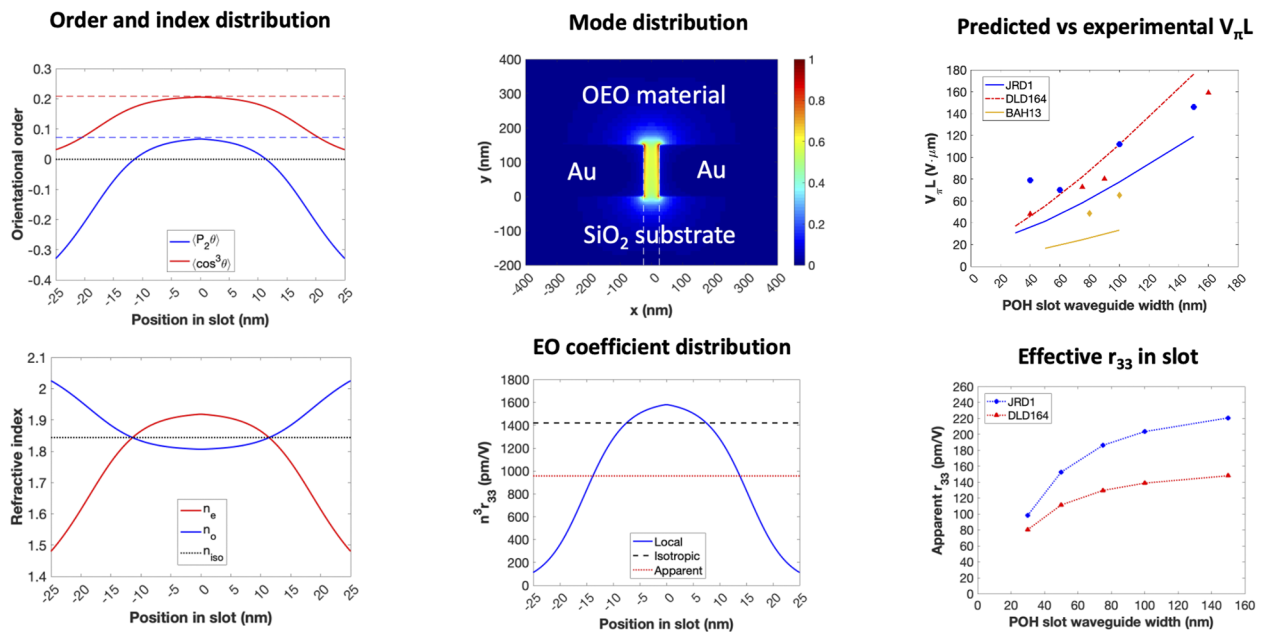


FIG. 4. Illustration of material property heterogeneity in a 50 nm slot waveguide POH device,¹¹ with reduced acentric and centrosymmetric order along the electric field axis (left), leading to a reduced material index along the axis of the mode and reduced Pockels response in the surface region where the mode in a plasmonic-organic hybrid device is most intense (center). The boundaries of the slot waveguide at ± 25 nm in the upper center figure are indicated by dashed white lines. As the surface region becomes a larger fraction of the total at narrower waveguide widths, modulation efficiency is expected to increase due to tighter confinement of the mode, but the effect is limited by the reduction in material EO performance due to reduced poling efficiency (right; chromophore structures shown in Fig. 6).^{10,11} Calculation of material performance from device $V_{\pi}L$ yields an apparent r_{33} averaged over the cross-section of the mode, which decreases for poled materials as waveguide width is reduced, leading to performance lagging expected performance if r_{33} retained its bulk value ("isotropic" line in the lower center panel).

field direction) due to interaction between chromophore dipoles and induced dipoles in the gold electrodes. The order along the poling field axis at the interface leads not only to a reduction in average EO activity in the waveguide but also to a mismatch between the regions of the highest optical field intensity and the highest electro-optic response. This information has motivated a reconsideration of sequential synthesis/self-assembly processing protocols, where covalent bonds between chromophores and electrodes support the organization of chromophores along the normal vector to the electrode surface.

Material processing utilizing sequential synthesis versus electric field poling.^{6,7,149–173} Sequential synthesis is a poling-free processing technique that deposits and covalently bonds aligned OEO molecules one monolayer at a time in a controlled fashion, building up to aligned chromophore multilayers (Fig. 5). The coupling chemistry to attach the layers is built upon established techniques for self-assembled monolayers,^{150,152,160,166,171} layer-by-layer deposition,^{13,156,167,172} click chemistry,^{158,174} and automated protein synthesis^{149,157} and is a solution-phase analog to fabrication processes such as atomic/molecular layer deposition, in which repeated applications of precursors enable high-quality conformal coatings.^{154,164,165,170,173}

The design of chromophores for sequential synthesis is inspired by prior work on OEO materials,^{154,161} nanostructured dielectric layers,¹⁶⁸ and surface grown polymers, as well as on our state-of-the-art, high β chromophores.^{17,128} Pioneering sequential

deposition of OEO materials was performed by the Katz and Marks groups.^{151,153–155,159,161,163,168,169} They developed a robust process to deposit aligned, low β OEO multilayers with a respectable EO coefficient of $r_{33} = 120$ pm/V at 1064 nm. However, three limitations kept this technology from being pursued further at the time: first, only relatively low β chromophores were used in these OEO multilayers, which resulted in lower EO coefficients than could be achieved with contemporary poled higher β materials. Second, OEO molecules have large dipole moments, and intermolecular repulsion at high densities reduces the maximum achievable order (Fig. 5, top left).¹⁶¹ Third, while high acentric order could be achieved in the initial layers, monolayer defects and the propagation of defect disorder had a multiplicative effect in thicker films, preventing the realization of effective EO activity for the hundreds of multilayers that were needed to span the $\sim 1\text{--}2$ μm spacing of mesoscale devices.¹⁵⁴ Such work, however, laid a good foundation for achieving high acentric order without poling, and the aforementioned limitations can be overcome by the strategies described below.

Modern high-performance chromophores such as JRD1¹⁷⁵ and BAH13¹⁷ (see Fig. 6 for the general structures of common chromophores) have more than an order of magnitude higher β than chromophores used in prior aligned multilayer sequential synthesis/self-assembly schemes, which enables dramatic improvements in performance.

However, high dipole moment molecules (JRD1 and BAH13 type chromophores have dipole moments in the 26–31 D range)

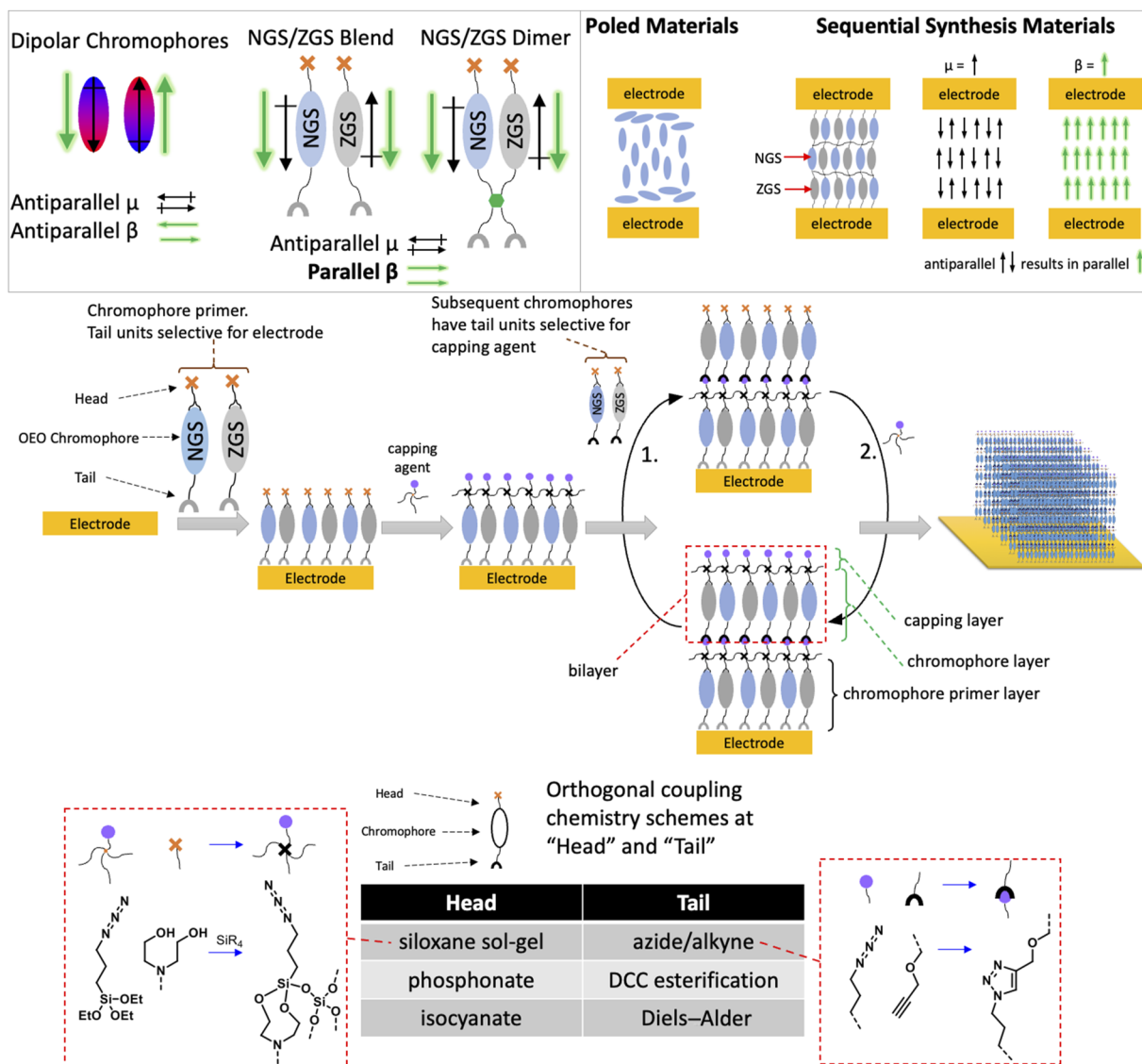


FIG. 5. (Top left) μ and β for single-component dipolar molecules, NGS/ZGS blends, and an NGS/ZGS dimer. (Top right) Comparison of alignment, μ , and β in narrow slot poled devices, and sequential synthesis materials. (Middle) Schematic illustration of a sequential synthesis protocol for a two-chromophore (NGS and ZGS) system. Various coupling chemistries are shown at the bottom of the figure.

tend to align in an antiparallel fashion when in close proximity (Fig. 5, top left), resulting in centrosymmetric ($\chi^2 = 0$) rather than acentric order ($\chi^2 > 0$). Prior molecular engineering of these chromophores—through the addition of sterically bulky side-chain groups—allows us to mask dipolar attraction, which enables efficient poling, achieving moderate acentric order as neat materials.^{20,128,134,175} While such molecular engineering techniques may be sufficient to improve acentric order in high dipole moment sequential synthesis layers, a better way to solve the dipole moment problem is to use a dual chromophore system consisting of neutral ground state (NGS) and zwitterionic ground state (ZGS)

chromophores (Fig. 5, top left and top right). NGS chromophores, such as our conventional chromophores, JRD1 and BAH13, have parallel dipole moments and β tensors. ZGS chromophores have antiparallel dipole moments and β tensors. Blending NGS and ZGS chromophores results in thermodynamically favored antiparallel dipole moment alignment and parallel (additive) β alignment (this antiparallel coupling of dipole moments is shown schematically as alternating blue and gray chromophores in Fig. 5).^{176,177}

Using model compounds, we have previously shown that this NGS/ZGS blending strategy produces Langmuir–Blodgett (LB) films

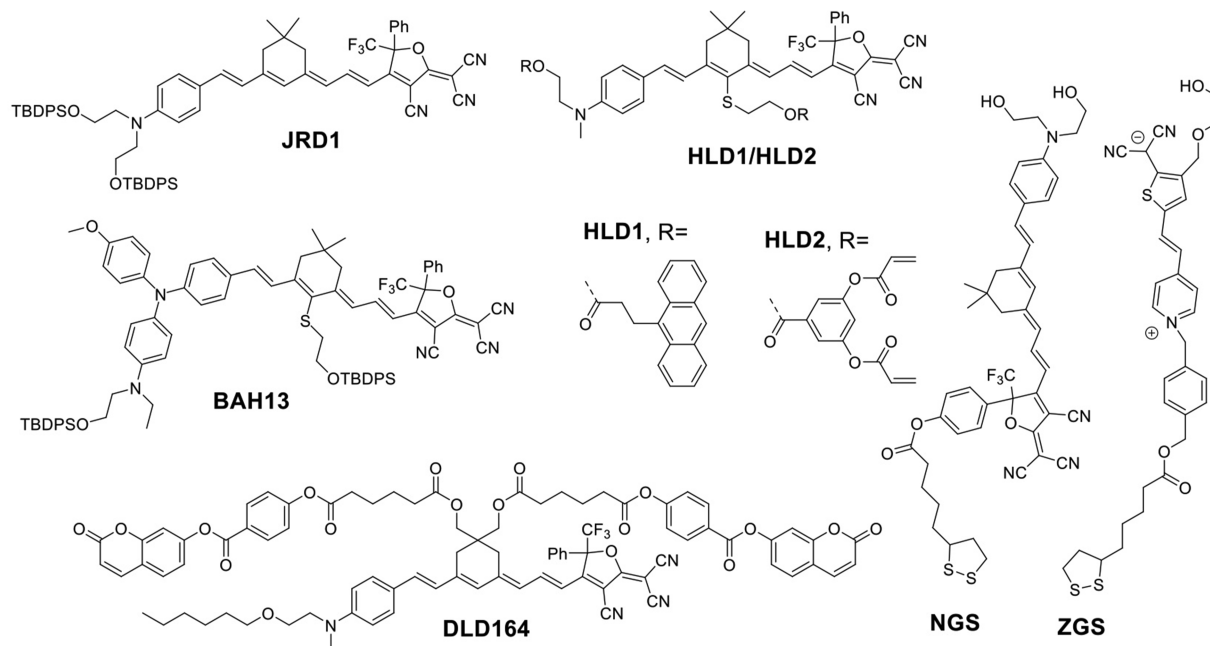


FIG. 6. Structures of some of the most common chromophores discussed are shown.

with better net alignment and acentric order than corresponding single component monolayers.^{7,176,177} While the LB technique shows a good way to circumvent the dipole repulsion problem, the LB method cannot be extended to a multilayer arrangement with net acentric hyperpolarizability order. Sequential synthesis, with covalent coupling, is necessary to control alignment layer to layer and retain it over a broad temperature range. Since the sequential synthesis is a solution process, dimerizing the NGS and ZGS chromophores (Fig. 5, top left) ensures that they reach the surface together and avoids potential phase separation in the monolayer, mitigating NGS/NGS and ZGS/ZGS antiparallel pairing in the solution that could result in slow monolayer formation rates and lower film quality.

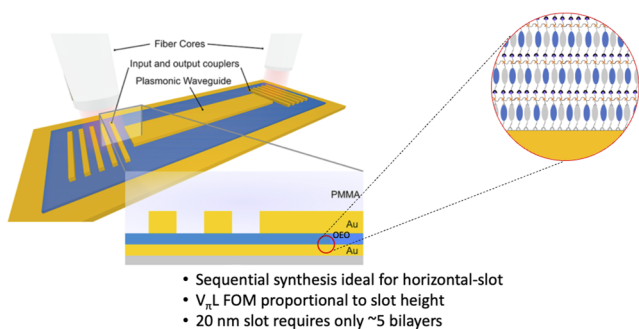


FIG. 7. Conceptual device design of a POH modulator implementing sequential synthesis of an OEO material based on a previously published horizontal waveguide POH device.⁹¹

Computational modeling, including DFT calculations for chromophore design and structure-property relationships as well as classical molecular dynamics for ordering and packing, can be used to fine tune the molecular structures and intermolecular interactions to optimize the acentric order in chromophore self-assembled monolayers. Several ZGS chromophores have been screened computationally thus far to identify ones that match well in dipole moment and β with leading NGS chromophores. Structural elements of the NGS and ZGS chromophore building blocks to be optimized include linker length (short or long), linker rigidity (aliphatic or aromatic), and attachment point to the acceptor, which impacts whether the molecule is linear or bent.

Following chromophore building block modeling of linkers and side chains to optimize acentric order, leading candidates are synthesized. Chromophore cores for sequential synthesis building blocks are based on previously synthesized high- β molecules such as JRD1 and BAH13. Next, the focus is on the coupling chemistry needed to build multilayers. Coupling chemistry is based on well-established self-assembled monolayer, molecular layer deposition (MLD), layer-by-layer deposition, click chemistry, sol-gel, metal/covalent organic framework, and solid phase peptide synthesis techniques. Like atomic layer deposition (ALD) and molecular layer deposition (MLD), sequential synthesis relies on two self-limiting surface reactions carried out sequentially, generating bilayers. To generate acentric alignment, the chromophore building blocks need to have different chemical coupling units on the “head” and “tail,” as shown schematically in Fig. 5. The tail unit is designed to selectively react with the electrode surface (or monolayer reactive surface groups for subsequent layers), generating a chromophore self-assembled monolayer (SAM). Sample NGS and ZGS

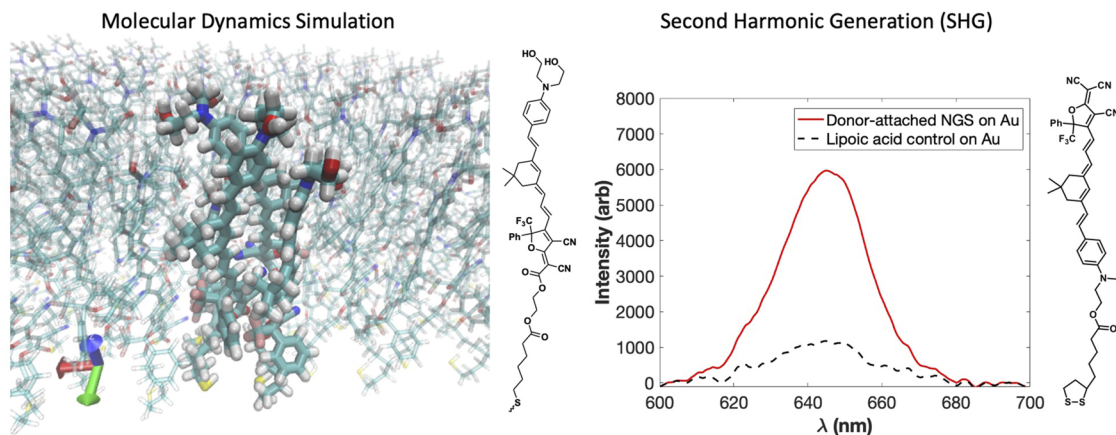


FIG. 8. (Left) Snapshot from molecular dynamics simulation of a chromophore-containing SAM, showing a side view of packing and an alignment and individual surface-attached chromophore. (Right) Second harmonic generation spectroscopy (SHG) of a donor-attached NGS chromophore monolayer and a control monolayer. SHG can be used to follow the growth of sequential synthesis layers and assess the acentric order.

chromophores capable of forming SAMs on gold are shown in Fig. 6, right. In a second subsequent reaction, the head unit reacts with a capping agent. These two reaction processes can be repeated multiple times to deposit bilayers (chromophore layer and capping layer). It is particularly attractive to develop this approach for nanophotonic devices because only a small number of sequential depositions are required. In modern POH devices, the electrode spacing has been as low as 40 nm, and even smaller is desired to reduce $V_{\pi L}$ (Fig. 7). For an electrode spacing of 20–40 nm, fewer than 10 chromophore layers are required; based on previous experiments, a high degree of acentric order is expected. While proof-of-concept chemistry and processing have been carried out, functional POH devices have not yet been demonstrated, although this is the next step.

The head and tail coupling chemistries of the sequential synthesis process need to be selective (orthogonal), high yielding, rapid, and compatible with each other. Fortunately, there are numerous proven click chemistry techniques from which to choose. Some examples of orthogonal pairs of click chemistry reactions that are compatible with NGS and ZGS chromophore synthesis and multilayer deposition are shown in the table of Fig. 5, bottom. Examples using siloxane coupling at the head and azide/alkyne coupling at the tail are shown in more detail. The capping layer presents a new functional group to bind the next chromophore building block. The chromophores will be much farther apart vertically than horizontally, so we believe there will be little dipole moment influence from the layer below on the exact position of each molecule in the new layer. The capping layer forms a 2D sheet, cross-linking the chromophores at the top (and bottom), giving it structural rigidity to provide high thermal stability for the acentric order. Similar materials (self-assembled nanodielectrics, SANDS¹⁶⁸) have thermal stability >675 K, suggesting that acentric order thermal stability of >475 K is achievable. If necessary, additional stability can be achieved by attaching crosslinking units to the bridge of the chromophores and conducting a crosslinking step (thermal or UV) after all chromophore layers have been deposited. With this addition, EO thermal stability >500 K is anticipated.

Simulation techniques remain important for these materials, additionally considering the impact of covalent bond restrictions on chromophore motion. The use of conventional MD approaches becomes much more viable. An example of chromophore monolayer organization from a classical MD calculation is shown in Fig. 8. The typical surface density of attachment units causes the chromophores to pack upright, perpendicular to the surface—an orientation leading to optimal EO activity.

SUMMARY OF CHANGES IN MATERIAL DESIGN AND FUTURE PROGNOSIS

The transition from mesoscale to nanoscale devices has forced a transformative change in material design and development, which has been greatly facilitated by improved computational and theoretical methods (see Fig. 9).

The overarching change in perspective is that material development and performance require understanding the device architectures in which those materials are incorporated. Independent consideration of materials and devices leads to confusion in comparisons of theory and experiment and poor guidance with respect to the development of materials and new device architectures. Optical nonlinearity depends on field intensities (field concentration) as well as the inherent hyperpolarizability and acentric order of fundamental material units. The ratio of materials at interfaces to materials in the bulk increases dramatically for nanophotonic device architectures, and this forces a change in perspective with respect to material synthesis and processing options, e.g., sequential synthesis vs electric field poling. However, it should also be kept in mind that electric field poling processing will continue to be the protocol of choice for certain device architectures (e.g., mesoscale devices and larger nanoscale devices). Insights gained from studies involving sequential synthesis are relevant to optimizing electrically-poled materials, and hybrid processing methodologies are likely to be developed.

Current research involving organic OEO materials largely focuses on the second and third generations, with materials routinely

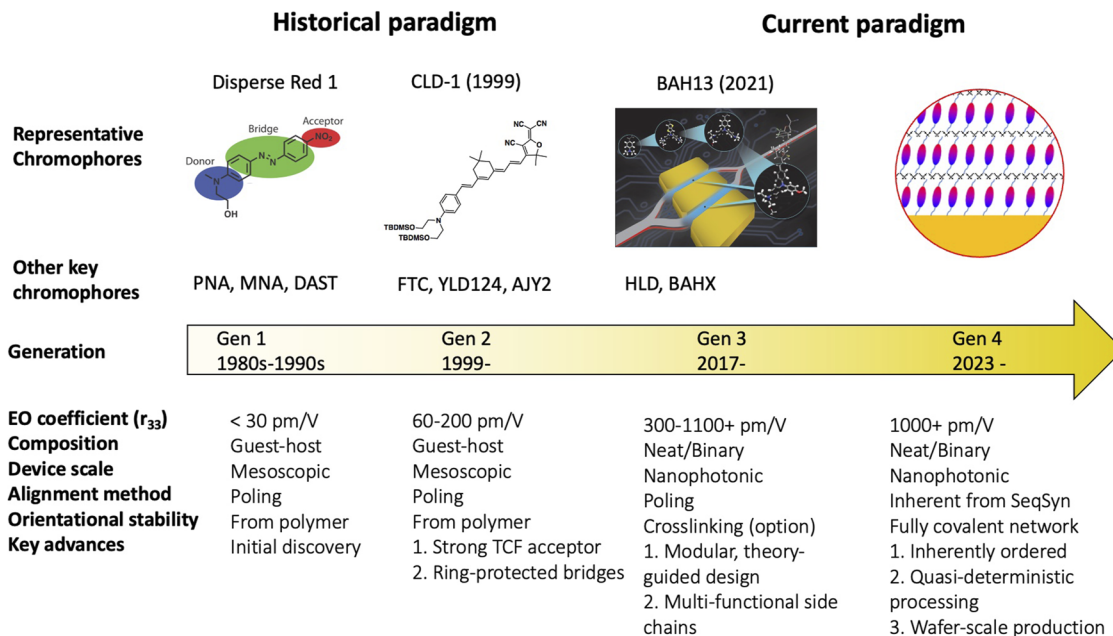


FIG. 9. The evolution of four generations of chromophores is illustrated. The first generation¹⁴³ involved azo dyes and stilbene derivatives in polymer hosts and typically had inferior performance to lithium niobate. The development of second-generation materials based around the tricyanovinylfuran (TCF) electron accepting moiety and extended, ring-locked bridges enabled performance on the order of 100 pm/V and initial polymer devices capable of sub-volt operation.¹⁷⁸ The late 2000s and early 2010s brought substantial examination of neat materials (no polymer host) for hybrid devices in which optical loss constraints were lessened.¹⁻³ These materials were initially limited due to low glass transition temperatures, which was remedied by high-glass transition (T_g) or covalently cross-linkable neat materials (third generation) in the late 2010s.^{128,179} This third generation was heavily derived from theory-guided design with an increased emphasis on modularity and high number density from multi-functional moieties. The next generation of OEO materials involves all-covalent architectures enabling performance greater than or equal to that of third generation materials, but in an even more stable, deterministically, and scalably processible manner.

yielding macroscopic EO activity values of several hundred pm/V,^{6,7,10,20,48,128,134,175,179-191} with exceptional materials yielding values more than 1000 pm/V.^{7,9,16,17} Substantial progress has been made in improving thermal^{6,9,48,52,128,192} and photochemical^{129,185} stability via crosslinking, yielding materials that surpass Telcordia standards.^{9,48,52,128,192} However, the marked attenuation of in-device EO activity in nanoscopic devices has driven fourth generation materials development to focus on sequential synthesis (Gen 4). Preliminary results based on the covalent coupling of chromophores to electrode surfaces show that ordered layers with a strong nonlinear response can be obtained with modern high-performance chromophores.⁷ The mixing of neutral ground state (NGS) and zwitterionic ground state (ZGS) chromophores provides a route to minimizing the effect of dipolar interactions of high hyperpolarizability chromophores.^{7,176,177} The covalent bonds of chromophores assembled by sequential synthesis should consistently yield in-device electro-optic values >1000 pm/V and thermal stability values on the order of chromophore decomposition temperatures (>500 K) rather than being limited by material glass transition temperature (<400 K) as is the case with electric field poling.⁶⁷ An improvement in photochemical stability is also to be expected.

The perspective related to the impact of material propagation loss on device optical insertion loss also changes dramatically with

the integration of materials into nanophotonic architectures—active material loss has meaning only relative to passive material loss. As optical nonlinearity is critical to the device lengths that can be utilized (voltage-length performance), a reconsideration of the optical nonlinearity/transparency (optical absorption loss) ratio becomes important. With improvement in the optical nonlinearity of Pockels effect materials, the attractiveness of hybrid integration of these materials vs semiconductor junction-based approaches changes dramatically. It is, however, important to keep in mind that there have been highly important advances for other materials (for example, transparent conducting oxides such as indium tin oxide)¹⁹³⁻¹⁹⁸ used for EO applications. Another emerging competitive material is graphene,^{94,118-124} and indeed, graphene is also emerging as an important electrode material for Pockels effect devices. A change in perspective with respect to material stability is required for nanophotonic architectures and new material processing options (e.g., crosslinking and sequential synthesis). In addition, the denser material matrices of materials prepared by sequential synthesis and crystal growth inhibit the in-diffusion of oxygen and moisture, leading to dramatically improved photostability.^{6,7} Although the glass transition temperatures realized with electric field poling materials permit Telcordia standards to be surpassed,¹⁹² greater temperature stability is required for certain applications. Sequential synthesis and/or crosslinking also improve mechanical

characteristics at reduced temperatures, particularly cryogenic temperatures. Cryogenic electro-optic operation has been demonstrated for a number of material types.^{127,199–208}

The improvements of in-device EO activity and thermal stability that are possible with sequential synthesis promise a significant improvement in $V_{\pi}L$, energy efficiency, bandwidth, and device footprint. The sequential synthesis should also permit a comparable improvement in optical rectification, dramatically improving the competitiveness of photodiodes based on electron excitation and charge generation.

An important event in the evolution of electronic/photonic integration has been the development of photonic foundry capability and increased access to these foundries by academic, government, and industrial researchers.⁷ While photonic foundries initially focused primarily on the integration of passive photonic circuitry (e.g., passive silicon photonics), this was rapidly followed by the development of active photonic devices such as germanium photodiodes and semiconductor junction modulators that enabled the creation of true photonic integrated circuits (PICs). The systematic optimization of these PICs enabled the current generation of silicon photonics products, such as optical transceivers for datacenter applications. More recently, the focus has turned to the integration of multiple materials technologies to enable performance beyond what is achievable in silicon photonics alone. The rapidly growing foundry ecosystem and the appearance of start-up companies focusing on silicon photonic hybrid and plasmonic hybrid technologies have been discussed elsewhere⁷ and promise a robust future for chip-scale integration of electronics and photonics.

Future prognosis for materials development and expansion of the application space. Future prognosis for R&D: Nanophotonic integration has dramatically influenced the size, weight, power, cost, and performance of information technology devices and is particularly impactful for airborne and satellite platforms. Nanophotonic EO device advances have already permitted modulation efficiencies ($V_{\pi}L$) to be improved to <0.04 V mm, bandwidths increased to THz frequencies, energy efficiencies to be improved to tens

of aJ/bit for digital signal processing, and device footprints to be reduced to $\sim 10 \mu\text{m}^2$, as well as achieving state-of-the-art spur free dynamics range (SFDR) and bit error ratio (BER) for analog and digital signal processing.⁷ Important for the implementation of nanophotonic technology have been the establishment of testbeds that permit the characterization of such small devices and foundry operations that permit the design and fabrication of such devices.⁷ In addition, the development of testbeds that permit R&D modeling of important applications such as fiber-wireless/free space telecommunication (see Fig. 10) and datacom systems has been important. In short, the implementation of R&D, fabrication, and testing infrastructure and electronic-photonic design automation (EPDA) software has started to come together and is (together with the growth of photonic foundries) dramatically accelerating technology development and implementation.

Expansion of the Application Space. The most important areas of initial focus for active nanophotonics involved data center interconnects and radio-over-fiber for defense and satellite communication applications.^{5,7,8,31–36,38–47,50–63,65–68,71–73,75,77,79,80} Improvements in datacom capacity have been critical for applications such as video, telemedicine, the Internet of Things (IoT), the metaverse, cloud computing, etc. Furthermore, scaling of datacom capability has required developments in nonlinear optical comb generation and a variety of EO device architectures as well as passive optical circuitry.

While the primary focus of OEO research has been on C-band ($1.55 \mu\text{m}$), datacom research motivates consideration of the O-band ($1.3 \mu\text{m}$) operation as well due to lower dispersion for short-range interconnects. Electro-optic sensor technology is growing rapidly in importance with its capability for sensing a wide range of physical and chemical phenomena.^{6,7} Embedded network sensing and point-of-care medical diagnosis are examples. Particularly noteworthy, LIDAR (especially when coupled with autonomous vehicle technology) is rapidly growing in importance and is being applied to fields ranging from environmental imaging and monitoring to agriculture, archeology, defense, and more.^{7,209–212} Spectroscopy has been significantly impacted, as has metrology involving ranging and

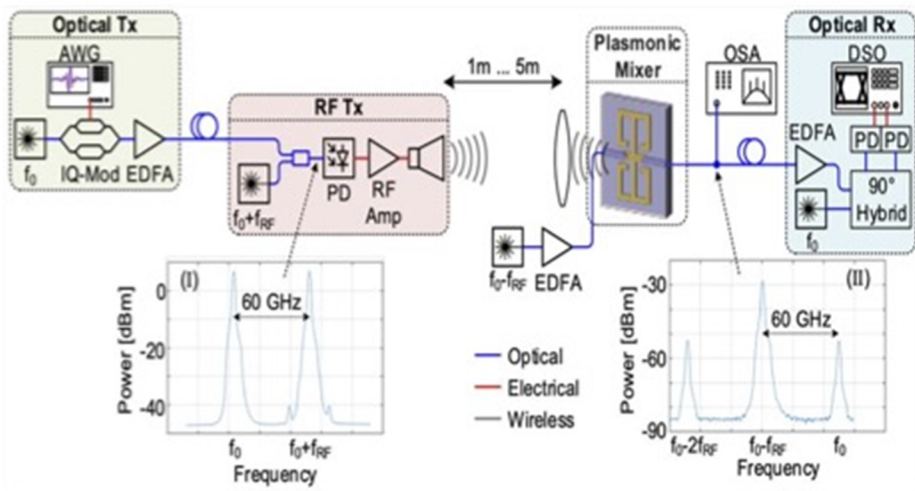


FIG. 10. Testbed for modeling fiber/wireless telecommunications. Critical components include the transmitter (Tx) and receiver (Rx) sections. Electro-optic elements consist of an IQ modulator in the Tx section and a resonant antenna in the Rx section. The high gain of the antenna facilitates the elimination of low noise amplifiers in the Rx section.^{7,78,92}

19 July 2023 12:40:07

imaging. Optical gyroscopes are seeing commercial applications.²¹³ The advent of hybrid active meta-surfaces has permitted transformative changes in display and sensor technologies exploiting the control of amplitude, phase, and polarization of light that is possible with such meta-surfaces.^{7,104} Meta-surfaces are also being applied to quantum technologies.¹¹⁵ In addition to these broader applications, a number of specific devices have been developed, including spatial light modulators, RF/millimeter wave beam steering (phased array radar), ultra-stable frequency generators (clocks), A/D converters, frequency shifters, acoustic spectrum analyzers, etc.^{6,7} Recently, interest has increased in the use of EO modulation for novel optical computing modalities, such as providing nonlinearity at the output stage of optical perceptions in neuromorphic analog optical computing.²¹⁴ Artificial intelligence/machine learning (AI/ML)²¹⁵ and quantum technologies represent additional emerging applications.

COMMENT ON OTHER MODULATION MATERIALS AND TECHNOLOGIES

Pockels effect modulation technology based on thin film lithium niobate (TFLN),^{216–221} thin-film barium titanate (BTO),²²² as well as EA modulation technologies²²³ based on conducting oxides such as indium tin oxide (ITO),^{193–198} merits comment. Competing with Pockels effect modulation are modulation techniques based on electro-absorption^{224–227} (including modulation based on graphene as well as inorganic materials) and carrier dispersion effects.^{53,224,228–231} Each of these approaches has advantages and disadvantages. TFLN has the advantage of low optical propagation loss and even lower absorption loss that extend from the visible to the infrared, as well as an extensive history of the use of bulk lithium niobate in telecom.^{58–60,103,106,109,111,114,115,199,216–221,224,228–231} Disadvantages include a small EO coefficient, a velocity mismatch between radio frequency and optical fields, and lithium-ion migration, which poses a concern for integration with CMOS electronics. Significant progress has been made with respect to addressing these limitations of TFLN technology, but the low EO coefficient (and hence large $V_{\pi}L$) limits the size of devices and the potential for dense integration with electronics. Recent progress with devices based on BTO has allowed them to realize small $V_{\pi}L$ values by capturing a large fraction of BTO's high (>900 pm/V) Pockels response,^{200,222} but they are limited in bandwidth and power consumption by BTO's high dielectric constant. EA based modulators can also realize exceptional $V_{\pi}L$ values, but demonstrations to date are often limited in bandwidth, loss, and power efficiency.²³²

Because of the rapid pace of improvement of all technologies, no tabular comparison of various technologies is presented, and the reader is referred to comparisons given in recent literature.^{8,57,61,224,225,228–231,233} The rapid pace of improvement of modulation and photodetection technologies is likely to continue with a corresponding expansion of applications. Different applications have different requirements with respect to operating wavelength range, operating temperature range, $V_{\pi}L$, bandwidth, energy efficiency, and size. No single material/device technology will be optimum for all applications. It can be noted that while the vast majority of OEO device research has focused on telecommunication wavelengths, visible wavelength devices can be achieved using shorter versions of high β chromophores.¹⁸⁴ A $V_{\pi}L$ of 5.2 V mm has

been demonstrated operating at a wavelength of 640 nm.¹⁸⁴ The relative competitiveness of various technologies for specific applications will likely continue to change with further research and development of individual technologies. The same can be said for material processing options and device architectures.

However, the opportunity for versatile design, synthesis, and processing options for organic second-order NLO materials suggests that the attractiveness of such materials will likely continue to increase, enhancing the performance and range of applications of hybrid silicon photonic, silicon nitride photonic, plasmonic, and meta-surface devices.

ACKNOWLEDGMENTS

ETH co-authors acknowledge partial support by ETH, aCryComm H2020-FETOPEN under Grant No. 899558, NEBULA H2020-ICT under Grant No. 871658, PlasmoniAC H2020-ICT under Grant No. 871391, plaCMOS H2020-ICT under Project No. 980997, and PLASILOR ERC under Grant No. 670478. Furthermore, ETH and Polariton acknowledge the aCryComm FETOPEN under Grant No. 899558. ETH and Polariton would like to acknowledge the support of the Binning and Rohrer Nanotechnology Center (BRNC), operated by IBM Research and ETH Zurich, Switzerland.

Dr. Christian Haffner (imec) acknowledges the funding by the European Union (ERC-2021-STG, Q-AMP, 101042414).

The UW co-authors gratefully acknowledge the financial support of the Air Force Office of Scientific Research (Grant No. FA9550-19-1-0069), the National Science Foundation (Grant Nos. DMR-13030800 and IIP-2036514), the University of Washington College of Arts and Sciences, and a DoD DURIP Grant (No. FA9550-21-1-0193). NLM co-authors gratefully acknowledge financial support from the National Science Foundation (Grant No. IIP-2036514) and NLM Photonics. Part of this work was conducted at the Molecular Analysis Facility, a National Nanotechnology Coordinated Infrastructure (NNCI) site at the University of Washington, which is supported in part by funds from the National Science Foundation (Award Nos. NNCI-2025489 and NNCI-1542101), the Molecular Engineering and Sciences Institute, and the Clean Energy Institute.

The authors thank Professor Alvin Kwiram for reading and editing this article.

AUTHOR DECLARATIONS

Conflict of Interest

Some work in this perspective is related to technology described in patent applications filed by the University of Washington (UW), including "Sequential Synthesis Technique for Deposition of Aligned Organic Electro-Optic Materials," US provisional application US 63/351,772, filed on behalf of UW and NLM Photonics (NLM), which is commercializing hybrid OEO technology. L.E.J. and D. L. E. are co-founders and part-time employees of NLM and equity holders in NLM. S.R.H. is a part-time employee of NLM and equity holder in NLM. B.H.R. is a co-founder, advisor to NLM, and an equity holder in NLM. The terms of this arrangement have been reviewed and approved by the University of Washington in accordance with its policies governing outside

work and financial conflicts of interest in research. B.B., C.H., and W.H. are co-founders, full-time employees, and equity holders in Polariton Technologies AG, which is commercializing POH technology. E.D.L and P.H. are full-time employees of Polariton Technologies AG. J.L. is an advisor to and equity holder in Polariton Technologies AG. All other authors declare no competing financial interests.

Author Contributions

All authors contributed to the preparation and editing of this article. Professor Dalton led the overall effort with assistance from Professor Leuthold. Figures 1–2, 4, and 9 were prepared by Dr. Lewis Johnson. Figures 3 and 6 were prepared by Dr. Delwin Elder. Figure 8 incorporates data from Drs. Johnson, Hammond, and Elder, as well as Professor Robinson. The preparation of the section on sequential synthesis was supervised by Dr. Elder with the assistance of Dr. Johnson. The preparation of the section on computational modeling was supervised by Dr. Johnson with the assistance of Professor Robinson.

L. R. Dalton: Conceptualization (equal); Formal analysis (equal); Funding acquisition (equal); Investigation (equal); Methodology (equal); Project administration (equal); Resources (equal); Supervision (equal); Validation (equal); Visualization (equal); Writing – original draft (lead); Writing – review & editing (lead). **J. Leuthold:** Conceptualization (equal); Data curation (equal); Formal analysis (equal); Funding acquisition (equal); Investigation (equal); Methodology (equal); Project administration (equal); Resources (equal); Supervision (equal); Validation (equal); Writing – original draft (supporting); Writing – review & editing (equal). **B. H. Robinson:** Conceptualization (equal); Data curation (equal); Formal analysis (equal); Funding acquisition (equal); Investigation (equal); Methodology (equal); Project administration (equal); Resources (equal); Software (equal); Supervision (equal); Validation (equal); Visualization (equal); Writing – original draft (supporting); Writing – review & editing (equal). **C. Haffner:** Conceptualization (equal); Data curation (equal); Formal analysis (equal); Investigation (equal); Methodology (equal); Project administration (equal); Resources (equal); Software (equal); Supervision (equal); Validation (equal); Writing – original draft (supporting); Writing – review & editing (equal). **D. L. Elder:** Conceptualization (equal); Data curation (equal); Formal analysis (equal); Funding acquisition (equal); Investigation (equal); Methodology (equal); Project administration (equal); Resources (equal); Supervision (equal); Validation (equal); Visualization (equal); Writing – original draft (supporting); Writing – review & editing (equal). **L. E. Johnson:** Conceptualization (equal); Data curation (equal); Formal analysis (equal); Funding acquisition (equal); Investigation (equal); Methodology (equal); Project administration (equal); Resources (equal); Software (equal); Supervision (equal); Validation (equal); Visualization (equal); Writing – original draft (supporting); Writing – review & editing (equal). **S. R. Hammond:** Data curation (equal); Formal analysis (equal); Investigation (equal); Methodology (equal); Resources (equal); Software (equal); Validation (equal); Visualization (equal); Writing – original draft (supporting); Writing – review & editing (equal). **W. Heni:** Conceptualization

(equal); Data curation (equal); Formal analysis (equal); Investigation (equal); Methodology (equal); Project administration (equal); Resources (equal); Supervision (equal); Validation (equal); Writing – original draft (supporting); Writing – review & editing (equal). **C. Hosessbacher:** Conceptualization (equal); Data curation (equal); Formal analysis (equal); Investigation (equal); Methodology (equal); Resources (equal); Validation (equal); Writing – original draft (supporting); Writing – review & editing (equal). **Benedikt Baeuerle:** Conceptualization (equal); Data curation (equal); Formal analysis (equal); Investigation (equal); Methodology (equal); Resources (equal); Validation (equal); Writing – original draft (supporting); Writing – review & editing (equal). **E. De Leo:** Data curation (equal); Formal analysis (equal); Investigation (equal); Methodology (equal); Resources (equal); Validation (equal); Writing – original draft (supporting); Writing – review & editing (equal). **U. Koch:** Conceptualization (equal); Data curation (equal); Formal analysis (equal); Investigation (equal); Methodology (equal); Resources (equal); Validation (equal); Writing – original draft (supporting); Writing – review & editing (equal). **P. Habegger:** Data curation (equal); Formal analysis (equal); Investigation (equal); Methodology (equal); Resources (equal); Validation (equal); Writing – original draft (supporting); Writing – review & editing (equal). **Y. Fedoryshyn:** Data curation (equal); Formal analysis (equal); Investigation (equal); Methodology (equal); Resources (equal); Validation (equal); Writing – original draft (supporting); Writing – review & editing (equal). **D. Moor:** Data curation (equal); Formal analysis (equal); Investigation (equal); Methodology (equal); Resources (equal); Validation (equal); Writing – original draft (supporting); Writing – review & editing (equal). **P. Ma:** Data curation (equal); Formal analysis (equal); Investigation (equal); Methodology (equal); Resources (equal); Validation (equal); Writing – original draft (supporting); Writing – review & editing (equal).

DATA AVAILABILITY

The data that support the findings of this study are available within the article.

REFERENCES

- ¹N. R. Council, *Optics and Photonics: Essential Technologies for Our Nation* (National Academies Press, Washington DC, 2013).
- ²G. Keeler, in *Workshop: Heterogeneous 3D Microsystems - Opportunities for Photonics: Emerging Computing Concepts and Architectures* (DARPA Electronics Resurgence Initiative Summit, 2020).
- ³G. Keeler, in *Optical Microsystem Technologies and Applications* (IEEE, San Francisco, 2021), Optical Fiber Communication.
- ⁴N. S. a. T. Council, *National Strategy for Advanced Manufacturing* (National Science and Technology Council, Washington DC, 2022).
- ⁵N. Margalit, C. Xiang, S. M. Bowers, A. Bjorlin, R. Blum, and J. E. Bowers, “Perspective on the future of silicon photonics and electronics,” *Appl. Phys. Lett.* **118**, 220501 (2021).
- ⁶L. R. Dalton, P. Gunter, M. Jazbinsek, O.-P. Kwon, and P. A. Sullivan, *Organic Electro-Optics and Photonics* (Cambridge University Press/Materials Research Society, Cambridge, UK, 2015).
- ⁷D. L. Elder and L. R. Dalton, “Organic electro-optics and optical rectification: From mesoscale to nanoscale hybrid devices and chip-scale integration of electronics and photonics,” *Ind. Eng. Chem. Res.* **61**, 1207–1231 (2022).

- ⁸W. Heni, Y. Kutuvantavida, C. Haffner, H. Zwickel, C. Kieninger, S. Wolf, M. Lauerermann, Y. Fedoryshyn, A. F. Tillack, L. E. Johnson, D. L. Elder, B. H. Robinson, W. Freude, C. Koos, J. Leuthold, and L. R. Dalton, "Silicon-organic and plasmonic-organic hybrid photonics," *ACS Photonics* **4**, 1576–1590 (2017).
- ⁹L. E. Johnson, D. L. Elder, H. Xu, S. W. Hammond, S. J. Benight, K. O'Malley, B. H. Robinson, and L. R. Dalton, "New paradigms in materials and devices for hybrid electro-optics and optical rectification," in *Molecular and Nano Machines IV*, edited by Z. Sekkat and T. Omatsu (SPIE, 2021).
- ¹⁰W. Heni, C. Haffner, D. L. Elder, A. F. Tillack, Y. Fedoryshyn, R. Cottier, Y. Salamin, C. Hoessbacher, U. Koch, B. Cheng, B. Robinson, L. R. Dalton, and J. Leuthold, "Nonlinearities of organic electro-optic materials in nanoscale slots and implications for the optimum modulator design," *Opt. Express* **25**, 2627 (2017).
- ¹¹L. E. Johnson, D. L. Elder, S. J. Benight, A. F. Tillack, S. R. Hammond, W. Heni, L. R. Dalton, and B. H. Robinson, "Birefringence, dimensionality, and surface influences on organic hybrid electro-optic performance," in D. Congreve, C. Nielsen, A. J. Musser, and D. Baran (Eds.) *Physical Chemistry of Semiconductor Materials and Interfaces XX* (SPIE, 2021).
- ¹²H. Xu, L. E. Johnson, Y. de Coene, D. L. Elder, S. R. Hammond, K. Clays, L. R. Dalton, and B. H. Robinson, "Bis(4-dialkylaminophenyl)heteroaryl amino donor chromophores exhibiting exceptional hyperpolarizabilities," *J. Mater. Chem. C* **9**, 2721–2728 (2021).
- ¹³M. S. Johal and L. E. v. d. L. Johnson, *Understanding Nanomaterials*. 2nd ed. (CRC Press, Taylor & Francis Group, Boca Raton, 2018), p. xxiv.
- ¹⁴L. R. Dalton, P. A. Sullivan, and D. H. Bale, "Electric field poled organic electro-optic materials: State of the art and future prospects," *Chem. Rev.* **110**, 25–55 (2010).
- ¹⁵B. H. Robinson, Y. Salamin, B. Baeuerle, A. Josten, M. Ayata, U. Koch, J. Leuthold, L. R. Dalton, L. E. Johnson, D. L. Elder, A. A. Kocherzhenko, C. M. Isborn, C. Haffner, W. Heni, C. Hoessbacher, and Y. Fedoryshyn, "Optimization of plasmonic-organic hybrid electro-optics," *J. Lightwave Technol.* **36**, 5036–5047 (2018).
- ¹⁶H. Xu, D. L. Elder, L. E. Johnson, Y. de Coene, S. R. Hammond, W. Vander Ghinst, K. Clays, L. R. Dalton, and B. H. Robinson, "Electro-optic activity in excess of 1000 pm/V achieved via theory-guided organic chromophore design," *Adv. Mater.* **33**, 2104174 (2021).
- ¹⁷H. Xu, D. L. Elder, L. E. Johnson, W. Heni, Y. de Coene, E. De Leo, M. Destraz, N. Meier, W. Vander Ghinst, S. R. Hammond, K. Clays, J. Leuthold, L. R. Dalton, and B. H. Robinson, "Design and synthesis of chromophores with enhanced electro-optic activities in both bulk and plasmonic-organic hybrid devices," *Mater. Horiz.* **9**, 261–270 (2022).
- ¹⁸A. F. Tillack, L. E. Johnson, M. Rawal, L. R. Dalton, and B. H. Robinson, "Modeling chromophore order: A guide for improving EO performance," *MRS Proc.* **1698**, 26 (2014).
- ¹⁹A. F. Tillack, L. E. Johnson, B. E. Eichinger, and B. H. Robinson, "Systematic generation of anisotropic coarse-grained Lennard-Jones potentials and their application to ordered soft matter," *J. Chem. Theory Comput.* **12**, 4362–4374 (2016).
- ²⁰A. F. Tillack and B. H. Robinson, "Toward optimal EO response from ONLO chromophores: A statistical mechanics study of optimizing shape," *J. Opt. Soc. Am. B* **33**, E121 (2016).
- ²¹T. Baehr-Jones, M. Hochberg, G. Wang, R. Lawson, Y. Liao, P. A. Sullivan, L. Dalton, A. K.-Y. Jen, and A. Scherer, "Optical modulation and detection in slotted Silicon waveguides," *Opt. Express* **13**, 5216 (2005).
- ²²T. Baehr-Jones, J. Witzens, and M. Hochberg, "Theoretical study of optical rectification at radio frequencies in a slot waveguide," *IEEE J. Quantum Electron.* **46**, 1634–1641 (2010).
- ²³C. Cox and E. Wooten, "Photodetection via optical rectification of terahertz-modulated optical carriers," *J. Lightwave Technol.* **39**, 7908–7914 (2021).
- ²⁴C. Koos, P. Vorreau, T. Vallaitis, P. Dumon, W. Bogaerts, R. Baets, B. Esembeson, I. Biaggio, T. Michinobu, F. Diederich, W. Freude, and J. Leuthold, "All-optical high-speed signal processing with silicon-organic hybrid slot waveguides," *Nat. Photonics* **3**, 216–219 (2009).
- ²⁵J. Leuthold, W. Freude, J.-M. Brosi, R. Baets, P. Dumon, I. Biaggio, M. L. Scimeca, F. Diederich, B. Frank, and C. Koos, "Silicon organic hybrid technology—A platform for practical nonlinear optics," *Proc. IEEE* **97**, 1304–1316 (2009).
- ²⁶R. Ding, T. Baehr-Jones, Y. Liu, R. Bojko, J. Witzens, S. Huang, J. Luo, S. Benight, P. Sullivan, J.-M. Fedeli, M. Fournier, L. Dalton, A. Jen, and M. Hochberg, "Demonstration of a low V_{π} L modulator with GHz bandwidth based on electro-optic polymer-clad silicon slot waveguides," *Opt. Express* **18**, 15618 (2010).
- ²⁷J. Leuthold, C. Koos, and W. Freude, "Nonlinear silicon photonics," *Nat. Photonics* **4**, 535–544 (2010).
- ²⁸H. Figi, D. H. Bale, A. Szep, L. R. Dalton, and A. Chen, "Electro-optic modulation in horizontally slotted silicon/organic crystal hybrid devices," *J. Opt. Soc. Am. B* **28**, 2291 (2011).
- ²⁹R. L. Nelson, R. S. Kim, A. Szep, N. G. Usechak, A. Chen, H. Sun, S. Shi, D. Abeysinghe, Y.-H. You, L. R. Dalton, D. W. Prather, C. Schuetz, and G. J. Schneider, "Fabrication and characterization of a hybrid SOI 1×4 silicon-slot optical modulator array incorporating EO polymers for optical phased-array antenna applications," in *RF and Millimeter-Wave Photonics II* (SPIE, 2012).
- ³⁰J. Leuthold, C. Koos, W. Freude, L. Alloatti, R. Palmer, D. Korn, J. Pfeifle, M. Lauerermann, R. Dinu, S. Wehrli, M. Jazbinsek, P. Gunter, M. Waldow, T. Wahlbrink, J. Bolten, H. Kurz, M. Fournier, J.-M. Fedeli, H. Yu, and W. Bogaerts, "Silicon-organic hybrid electro-optical devices," *IEEE J. Sel. Top. Quantum Electron.* **19**, 114–126 (2013).
- ³¹L. Alloatti, R. Palmer, S. Diebold, K. P. Pahl, B. Chen, R. Dinu, M. Fournier, J.-M. Fedeli, T. Zwick, W. Freude, C. Koos, and J. Leuthold, "100 GHz silicon-organic hybrid modulator," *Light: Sci. Appl.* **3**, e173 (2014).
- ³²M. Lauerermann, R. Palmer, S. Koeber, P. C. Schindler, D. Korn, T. Wahlbrink, J. Bolten, M. Waldow, D. L. Elder, L. R. Dalton, J. Leuthold, W. Freude, and C. Koos, "Low-power silicon-organic hybrid (SOH) modulators for advanced modulation formats," *Opt. Express* **22**, 29927 (2014).
- ³³R. Palmer, W. Freude, J. Leuthold, C. Koos, S. Koeber, D. L. Elder, M. Woessner, W. Heni, D. Korn, M. Lauerermann, W. Bogaerts, and L. Dalton, "High-speed, low drive-voltage silicon-organic hybrid modulator based on a binary-chromophore electro-optic material," *J. Lightwave Technol.* **32**, 2726–2734 (2014).
- ³⁴C. Weimann, P. C. Schindler, R. Palmer, S. Wolf, D. Bekele, D. Korn, J. Pfeifle, S. Koeber, R. Schmogrow, L. Alloatti, D. Elder, H. Yu, W. Bogaerts, L. R. Dalton, W. Freude, J. Leuthold, and C. Koos, "Silicon-organic hybrid (SOH) frequency comb sources for terabit/s data transmission," *Opt. Express* **22**, 3629 (2014).
- ³⁵S. Koeber, R. Palmer, M. Lauerermann, W. Heni, D. L. Elder, D. Korn, M. Woessner, L. Alloatti, S. Koenig, P. C. Schindler, H. Yu, W. Bogaerts, L. R. Dalton, W. Freude, J. Leuthold, and C. Koos, "Femtjoule electro-optic modulation using a silicon-organic hybrid device," *Light: Sci. Appl.* **4**, e255 (2015).
- ³⁶M. Lauerermann, S. Wolf, P. C. Schindler, R. Palmer, S. Koeber, D. Korn, L. Alloatti, T. Wahlbrink, J. Bolten, M. Waldow, M. Koenigsmann, M. Kohler, D. Malsam, D. L. Elder, P. V. Johnston, N. Phillips-Sylvain, P. A. Sullivan, L. R. Dalton, J. Leuthold, W. Freude, and C. Koos, "40 Gb/s 16QAM signaling at 160 Gb/s in a silicon-organic hybrid modulator," *J. Lightwave Technol.* **33**, 1210–1216 (2015).
- ³⁷M. Lauerermann, C. Weimann, A. Knopf, W. Heni, R. Palmer, S. Koeber, D. L. Elder, W. Bogaerts, J. Leuthold, L. R. Dalton, C. Rembe, W. Freude, and C. Koos, "Integrated optical frequency shifter in silicon-organic hybrid (SOH) technology," *Opt. Express* **24**, 11694 (2016).
- ³⁸M. R. Billah, J. N. Kemal, P. Marin-Palomo, M. Blaicher, Y. Kutuvantavida, C. Kieninger, H. Zwickel, P.-I. Dietrich, S. Wolf, T. Hoose, Y. Xu, U. Tropfenz, M. Moehle, S. Randel, W. Freude, and C. Koos, "Four-Channel 784 Gbit/s transmitter module enabled by photonic wire bonding and silicon-organic hybrid modulators," in *2017 European Conference on Optical Communication (ECOC)* (Optica, 2017), pp. 1–3.
- ³⁹H. Zwickel, T. D. Keulenaer, S. Wolf, C. Kieninger, Y. Kutuvantavida, M. Lauerermann, M. Verplaetse, R. Pierco, R. Vaernewyck, A. Vyncke, X. Yin, G. Torfs, W. Freude, E. Mentovich, J. Bauwelinck, and C. Koos, "100 Gbit/s serial transmission using a silicon-organic hybrid (SOH) modulator and a duobinary driver IC," in *Optical Fiber Communications Conference (OFC)*, 2017.
- ⁴⁰H. Zwickel, S. Wolf, C. Kieninger, Y. Kutuvantavida, M. Lauerermann, T. de Keulenaer, A. Vyncke, R. Vaernewyck, J. Luo, A. K.-Y. Jen, W. Freude,

- J. Bauwelinck, S. Randel, and C. Koos, "Silicon-organic hybrid (SOH) modulators for intensity-modulation/direct-detection links with line rates of up to 120 Gbit/s," *Opt. Express* **25**, 23784 (2017).
- ⁴¹C. Kieninger, Y. Kutuvantavida, H. Miura, J. N. Kemal, H. Zwickel, F. Qiu, M. Lauerermann, W. Freude, S. Randel, S. Yokoyama, and C. Koos, "Demonstration of long-term thermally stable silicon-organic hybrid modulators at 85 °C," *Opt. Express* **26**, 27955 (2018).
- ⁴²C. Kieninger, Y. Kutuvantavida, D. L. Elder, S. Wolf, H. Zwickel, M. Blaicher, J. N. Kemal, M. Lauerermann, S. Randel, W. Freude, L. R. Dalton, and C. Koos, "Ultra-high electro-optic activity demonstrated in a silicon-organic hybrid modulator," *Optica* **5**, 739–748 (2018).
- ⁴³S. Wolf, H. Zwickel, W. Hartmann, M. Lauerermann, Y. Kutuvantavida, C. Kieninger, L. Altenhain, R. Schmid, J. Luo, A. K.-Y. Jen, S. Randel, W. Freude, and C. Koos, "Silicon-organic hybrid (SOH) mach-Zehnder modulators for 100 Gbit/s on-off keying," *Sci. Rep.* **8**, 2598 (2018).
- ⁴⁴S. Wolf, H. Zwickel, C. Kieninger, M. Lauerermann, W. Hartmann, Y. Kutuvantavida, W. Freude, S. Randel, and C. Koos, "Coherent modulation up to 100 GBd 16QAM using silicon-organic hybrid (SOH) devices," *Opt. Express* **26**, 220 (2018).
- ⁴⁵H. Zwickel, J. N. Kemal, C. Kieninger, Y. Kutuvantavida, J. Rittershofer, M. Lauerermann, W. Freude, S. Randel, and C. Koos, "Electrically packaged silicon-organic hybrid (SOH) I/Q-modulator for 64 GBd operation," *Opt. Express* **26**, 34580 (2018).
- ⁴⁶C. Kieninger, C. Füllner, H. Zwickel, Y. Kutuvantavida, J. N. Kemal, C. Eschenbaum, D. L. Elder, L. R. Dalton, W. Freude, S. Randel, and C. Koos, "SOH Mach-Zehnder modulators for 100 GBd PAM4 signaling with sub-1 dB phase-shifter loss," in *Optical Fiber Communication Conference (OFC)* (2020), 2020.
- ⁴⁷C. Kieninger, C. Füllner, H. Zwickel, Y. Kutuvantavida, J. N. Kemal, C. Eschenbaum, D. L. Elder, L. R. Dalton, W. Freude, S. Randel, and C. Koos, "Silicon-organic hybrid (SOH) Mach-Zehnder modulators for 100 GBd PAM4 signaling with sub-1 dB phase-shifter loss," *Opt. Express* **28**, 24693 (2020).
- ⁴⁸G.-W. Lu, J. Hong, F. Qiu, A. M. Spring, T. Kashino, J. Oshima, M.-a. Ozawa, H. Nawata, and S. Yokoyama, "High-temperature-resistant silicon-polymer hybrid modulator operating at up to 200 Gbit s⁻¹ for energy-efficient datacentres and harsh-environment applications," *Nat. Commun.* **11**, 4224 (2020).
- ⁴⁹H. Zwickel, S. Singer, C. Kieninger, Y. Kutuvantavida, N. Muradyan, T. Wahlbrink, S. Yokoyama, S. Randel, W. Freude, and C. Koos, "Verified equivalent-circuit model for slot-waveguide modulators," *Opt. Express* **28**, 12951 (2020).
- ⁵⁰S. Ummethala, J. N. Kemal, A. S. Alam, M. Lauerermann, A. Kuzmin, Y. Kutuvantavida, S. H. Nandam, L. Hahn, D. L. Elder, L. R. Dalton, T. Zwick, S. Randel, W. Freude, and C. Koos, "Hybrid electro-optic modulator combining silicon photonic slot waveguides with high-k radio-frequency slotlines," *Optica* **8**, 511 (2021).
- ⁵¹I. Taghavi, M. Moridsadat, A. Tofini, S. Raza, N. A. F. Jaeger, L. Chrostowski, B. J. Shastri, and S. Shekhar, "Polymer modulators in silicon photonics: Review and projections," *Nanophotonics* **11**, 3855–3871 (2022).
- ⁵²C. Eschenbaum, A. Mertens, C. Fullner, A. Kuzmin, A. Schwarzenberger, A. Kotz, G. Ramann, M. Chen, J. Drisko, B. Johnson, J. Zyskind, J. Marcelli, M. Leppy, W. Freude, S. Randel, and C. Koos, "Thermally stable silicon-organic hybrid (SOH) mach-Zehnder modulator for 140 GBd PAM4 transmission with sub-1 V drive signals," in *European Conference on Optical Communications (ECOC)*, 2022.
- ⁵³Y. Li, Y. Zhang, L. Zhang, and A. W. Poon, "Silicon and hybrid silicon photonic devices for intra-datacenter applications: State of the art and perspectives [Invited]," *Photonics Res.* **3**, B10 (2015).
- ⁵⁴X. Wang, P. O. Weigel, J. Zhao, M. Ruesing, and S. Mookherjea, "Achieving beyond-100-GHz large-signal modulation bandwidth in hybrid silicon photonics Mach Zehnder modulators using thin film lithium niobate," *APL Photonics* **4**, 096101 (2019).
- ⁵⁵D. Zhu, L. Shao, M. Yu, R. Cheng, B. Desiatov, C. J. Xin, Y. Hu, J. Holzgrafe, S. Ghosh, A. Shams-Ansari, E. Puma, N. Sinclair, C. Reimer, M. Zhang, and M. Lončar, "Integrated photonics on thin-film lithium niobate," *Adv. Opt. Photonics* **13**, 242 (2021).
- ⁵⁶G. Chen, K. Chen, R. Gan, Z. Ruan, Z. Wang, P. Huang, C. Lu, A. P. T. Lau, D. Dai, C. Guo, and L. Liu, "High performance thin-film lithium niobate modulator on a silicon substrate using periodic capacitively loaded traveling-wave electrode," *APL Photonics* **7**, 026103 (2022).
- ⁵⁷K. Li, D. Thomson, S. Liu, W. Zhang, W. Cao, C. Littlejohns, X. Yan, M. Ebert, M. Banakar, D. Tran, F. Meng, H. Du, and G. Reed, "112G baud sub pJ/bit integrated CMOS-silicon photonics transmitter," Research Square, 2022.
- ⁵⁸J. Mao, H. Sato, G.-W. Lu, and S. Yokoyama, "Heterogeneous silicon-on-lithium niobate electro-optic modulator for 100-Gbaud modulation," *APL Photonics* **7**, 126103 (2022).
- ⁵⁹F. Valdez, V. Mere, X. Wang, N. Boynton, T. A. Friedmann, S. Arterburn, C. Dallo, A. T. Pomerene, A. L. Starbuck, D. C. Trotter, A. L. Lentine, and S. Mookherjea, "110 GHz, 110 mW hybrid silicon-lithium niobate Mach-Zehnder modulator," *Sci. Rep.* **12**, 18611 (2022).
- ⁶⁰F. Valdez, V. Mere, X. Wang, and S. Mookherjea, "Integrated O- and C-band silicon-lithium niobate mach-Zehnder modulators with 100 GHz bandwidth, low voltage, and low loss," *Opt. Express* **31**, 5273–5289 (2023).
- ⁶¹C. Koos, J. Leuthold, W. Freude, M. Kohl, L. Dalton, W. Bogaerts, A. L. Giesecke, M. Lauerermann, A. Melikyan, S. Koeber, S. Wolf, C. Weimann, S. Muehlbrandt, K. Koehnle, J. Pfeifle, W. Hartmann, Y. Kutuvantavida, S. Ummethala, R. Palmer, D. Korn, L. Alloatti, P. C. Schindler, D. L. Elder, T. Wahlbrink, and J. Bolten, "Silicon-organic hybrid (SOH) and plasmonic-organic hybrid (POH) integration," *J. Lightwave Technol.* **34**, 256–268 (2016).
- ⁶²C. Koos, W. Freude, J. Leuthold, L. R. Dalton, S. Wolf, S. Muehlbrandt, A. Melikyan, H. Zwickel, T. Harter, Y. Kutuvantavida, C. Kieninger, M. Lauerermann, and D. Elder, "Nanophotonic modulators and photodetectors using silicon photonic and plasmonic device concepts," in *Proceedings of SPIE*, edited by B. Witzigmann, M. Osinski, and Y. Arakawa (SPIE, 2017).
- ⁶³S. Ummethala, *Plasmonic-Organic and Silicon-Organic Hybrid Modulators for High-Speed Signal Processing* (Doctor of Engineering, Karlsruhe Institute of Technology, 2021).
- ⁶⁴S.-K. Kim, N. Sylvain, S. J. Benight, I. Kosilkina, D. H. Bale, B. H. Robinson, J. Park, K. Geary, A. K. Jen, W. H. Steier, H. R. Fetterman, P. Berini, L. R. Dalton, W. H. Steier, H. R. Fetterman, P. Berini, and L. R. Dalton, "Active plasmonic and metamaterials and devices," in *Metamaterials: Fundamentals and Applications III* (SPIE, 2010).
- ⁶⁵C. Haffner, W. Heni, Y. Fedoryshyn, J. Niegemann, A. Melikyan, D. L. Elder, B. Baeuerle, Y. Salamin, A. Josten, U. Koch, C. Hoessbacher, F. Ducry, L. Juchli, A. Emboras, D. Hillerkuss, M. Kohl, L. R. Dalton, C. Hafner, and J. Leuthold, "All-plasmonic Mach-Zehnder modulator enabling optical high-speed communication at the microscale," *Nat. Photonics* **9**, 525–528 (2015).
- ⁶⁶W. Heni, C. Hoessbacher, C. Haffner, Y. Fedoryshyn, B. Baeuerle, A. Josten, D. Hillerkuss, Y. Salamin, R. Bonjour, A. Melikyan, M. Kohl, D. L. Elder, L. R. Dalton, C. Hafner, and J. Leuthold, "High speed plasmonic modulator array enabling dense optical interconnect solutions," *Opt. Express* **23**, 29746 (2015).
- ⁶⁷J. Leuthold, C. Haffner, W. Heni, C. Hoessbacher, J. Niegemann, Y. Fedoryshyn, A. Emboras, C. Hafner, A. Melikyan, M. Kohl, D. L. Elder, L. R. Dalton, and I. Tomkos, "Plasmonic devices for communications," in *2015 17th International Conference on Transparent Optical Networks (ICTON)* (IEEE, 2015), pp. 1–3.
- ⁶⁸A. Melikyan, K. Koehnle, M. Lauerermann, R. Palmer, S. Koeber, S. Muehlbrandt, P. C. Schindler, D. L. Elder, S. Wolf, W. Heni, C. Haffner, Y. Fedoryshyn, D. Hillerkuss, M. Sommer, L. R. Dalton, D. Van Thourhout, W. Freude, M. Kohl, J. Leuthold, and C. Koos, "Plasmonic-organic hybrid (POH) modulators for OOK and BPSK signaling at 40 Gbit/s," *Opt. Express* **23**, 9938 (2015).
- ⁶⁹Y. Salamin, W. Heni, C. Haffner, Y. Fedoryshyn, C. Hoessbacher, R. Bonjour, M. Zahner, D. Hillerkuss, P. Leuchtmann, D. L. Elder, L. R. Dalton, C. Hafner, and J. Leuthold, "Direct conversion of free space millimeter waves to optical domain by plasmonic modulator antenna," *Nano Lett.* **15**, 8342–8346 (2015).
- ⁷⁰R. Bonjour, M. Burla, F. C. Abrecht, S. Welschen, C. Hoessbacher, W. Heni, S. A. Gebrewold, B. Baeuerle, A. Josten, Y. Salamin, C. Haffner, P. V. Johnston, D. L. Elder, P. Leuchtmann, D. Hillerkuss, Y. Fedoryshyn, L. R. Dalton, C. Hafner, and J. Leuthold, "Plasmonic phased array feeder enabling ultra-fast beam steering at millimeter waves," *Opt. Express* **24**, 25608 (2016).
- ⁷¹C. Haffner, W. Heni, Y. Fedoryshyn, A. Josten, B. Baeuerle, C. Hoessbacher, Y. Salamin, U. Koch, N. Dordevic, P. Mousel, R. Bonjour, A. Emboras, D. Hillerkuss, P. Leuchtmann, D. L. Elder, L. R. Dalton, C. Hafner, and J. Leuthold, "Plasmonic organic hybrid modulators—scaling highest speed photonics to the microscale," *Proc. IEEE* **104**, 2362–2379 (2016).

- ⁷²W. Heni, C. Haffner, B. Baeuerle, Y. Fedoryshyn, A. Josten, D. Hillerkuss, J. Niegemann, A. Melikyan, M. Kohl, D. L. Elder, L. R. Dalton, C. Haffner, and J. Leuthold, “108 Gbit/s plasmonic Mach-Zehnder modulator with >70-GHz electrical bandwidth,” *J. Lightwave Technol.* **34**, 393–400 (2016).
- ⁷³M. Ayata, Y. Fedoryshyn, W. Heni, B. Baeuerle, A. Josten, D. L. Elder, L. R. Dalton, and J. Leuthold, “Complete high-speed plasmonic modulator in a single metal layer,” *Science* **358**, 630–632 (2017).
- ⁷⁴C. Haffner, W. Heni, D. L. Elder, Y. Fedoryshyn, N. Đorđević, D. Chelladurai, U. Koch, K. Portner, M. Burla, B. Robinson, L. R. Dalton, and J. Leuthold, “Harnessing nonlinearities near material absorption resonances for reducing losses in plasmonic modulators,” *Opt. Mater. Express* **7**, 2168 (2017).
- ⁷⁵C. Hoessbacher, A. Josten, B. Baeuerle, Y. Fedoryshyn, H. Hettrich, Y. Salamin, W. Heni, C. Haffner, C. Kaiser, R. Schmid, D. L. Elder, D. Hillerkuss, M. Möller, L. R. Dalton, and J. Leuthold, “Plasmonic modulator with >170 GHz bandwidth demonstrated at 100 GbD NRZ,” *Opt. Express* **25**, 1762 (2017).
- ⁷⁶C. Haffner, “Non-resonant and resonant surface plasmon polariton modulators for optical communications,” in *Doctor of Sciences* (ETH, Zurich, 2018).
- ⁷⁷C. Haffner, D. Chelladurai, Y. Fedoryshyn, A. Josten, B. Baeuerle, W. Heni, T. Watanabe, T. Cui, B. Cheng, S. Saha, D. L. Elder, L. R. Dalton, A. Boltasseva, V. M. Shalaev, N. Kinsey, and J. Leuthold, “Low-loss plasmon-assisted electro-optic modulator,” *Nature* **556**, 483–486 (2018).
- ⁷⁸Y. Salamin, B. Baeuerle, W. Heni, F. C. Abrecht, A. Josten, Y. Fedoryshyn, C. Haffner, R. Bonjour, T. Watanabe, M. Burla, D. L. Elder, L. R. Dalton, and J. Leuthold, “Microwave plasmonic mixer in a transparent fibre-wireless link,” *Nat. Photonics* **12**, 749–753 (2018).
- ⁷⁹M. Ayata, D. L. Elder, L. R. Dalton, J. Leuthold, Y. Fedoryshyn, W. Heni, A. Josten, B. Baeuerle, C. Haffner, C. Hoessbacher, U. Koch, and Y. Salamin, “All-plasmonic IQ modulator with a 36 μm fiber-to-fiber pitch,” *J. Lightwave Technol.* **37**, 1492–1497 (2019).
- ⁸⁰B. Baeuerle, W. Heni, C. Hoessbacher, Y. Fedoryshyn, A. Josten, C. Haffner, T. Watanabe, C. Uhl, H. Hettrich, D. L. Elder, L. R. Dalton, M. Moller, and J. Leuthold, “Reduced equalization needs of 100 GHz bandwidth plasmonic modulators,” *J. Lightwave Technol.* **37**, 2050–2057 (2019).
- ⁸¹B. Baeuerle, W. Heni, C. Hoessbacher, Y. Fedoryshyn, U. Koch, A. Josten, T. Watanabe, C. Uhl, H. Hettrich, D. L. Elder, L. R. Dalton, M. Möller, and J. Leuthold, “120 GbD plasmonic Mach-Zehnder modulator with a novel differential electrode design operated at a peak-to-peak drive voltage of 178 mV,” *Opt. Express* **27**, 16823 (2019).
- ⁸²M. Burla, C. Hoessbacher, W. Heni, C. Haffner, Y. Fedoryshyn, D. Werner, T. Watanabe, H. Massler, D. L. Elder, L. R. Dalton, and J. Leuthold, “500 GHz plasmonic Mach-Zehnder modulator enabling sub-THz microwave photonics,” *APL Photonics* **4**, 056106 (2019).
- ⁸³U. Koch, L. R. Dalton, J. Leuthold, A. Messner, C. Hoessbacher, W. Heni, A. Josten, B. Baeuerle, M. Ayata, Y. Fedoryshyn, and D. L. Elder, “Ultra-compact terabit plasmonic modulator array,” *J. Lightwave Technol.* **37**, 1484–1491 (2019).
- ⁸⁴D. Hillerkuss, M. Burla, Y. Salamin, R. Bonjour, C. Hoessbacher, C. Haffner, W. Heni, Y. Fedoryshyn, D. Werner, B. Baeuerle, A. Josten, T. Watanabe, D. Elder, L. Dalton, J. Leuthold, F. Abrecht, Y. Salamin, M. Burla, and D. Hillerkuss, “Integrated photonic and plasmonic technologies for microwave signal processing enabling mm-wave and sub-THz wireless communication systems,” in *Broadband Access Communication Technologies XIII*, 2019.
- ⁸⁵Y. Salamin, I.-C. Benea-Chelms, Y. Fedoryshyn, W. Heni, D. L. Elder, L. R. Dalton, J. Faist, and J. Leuthold, “Compact and ultra-efficient broadband plasmonic terahertz field detector,” *Nat. Commun.* **10**, 5550 (2019).
- ⁸⁶B. Baeuerle, C. Hoessbacher, W. Heni, Y. Fedoryshyn, U. Koch, A. Josten, D. L. Elder, L. R. Dalton, and J. Leuthold, “100 GbD IM/DD transmission over 14 km SMF in the C-band enabled by a plasmonic SSB MZM,” *Opt. Express* **28**, 8601–8608 (2020).
- ⁸⁷I.-C. Benea-Chelms, Y. Salamin, F. F. Settembrini, Y. Fedoryshyn, W. Heni, D. L. Elder, L. R. Dalton, J. Leuthold, and J. Faist, “Electro-optic interface for ultrasensitive intracavity electric field measurements at microwave and terahertz frequencies,” *Optica* **7**, 498 (2020).
- ⁸⁸M. Burla, C. Hoessbacher, W. Heni, C. Haffner, Y. Fedoryshyn, D. Werner, T. Watanabe, Y. Salamin, H. Massler, D. Hillerkuss, D. Elder, L. Dalton, J. Leuthold, B. B. Dingel, K. Tsukamoto, and S. Mikroulis, “Novel applications of plasmonics and photonics devices to sub-THz wireless,” in *Broadband Access Communication Technologies XIV*, 2020.
- ⁸⁹W. Heni, B. Baeuerle, H. Mardoyan, F. Jorge, J. M. Estaran, A. Konczykowska, M. Riet, B. Duval, V. Nodjiadjim, M. Goix, J.-Y. Dupuy, M. Destraz, C. Hoessbacher, Y. Fedoryshyn, H. Xu, D. L. Elder, L. R. Dalton, J. Renaudier, and J. Leuthold, “Ultra-high-speed 2:1 digital selector and plasmonic modulator IM/DD transmitter operating at 222 GBaud for intra-datacenter applications,” *J. Lightwave Technol.* **38**, 2734 (2020).
- ⁹⁰U. Koch, C. Uhl, H. Hettrich, Y. Fedoryshyn, C. Hoessbacher, W. Heni, B. Baeuerle, B. I. Bitachon, A. Josten, M. Ayata, H. Xu, D. L. Elder, L. R. Dalton, E. Mentovich, P. Bakopoulos, S. Lischke, A. Krüger, L. Zimmermann, D. Tsiokos, N. Pleros, M. Möller, and J. Leuthold, “A monolithic bipolar CMOS electronic-plasmonic high-speed transmitter,” *Nat. Electron.* **3**, 338 (2020).
- ⁹¹A. Messner, P. A. Jud, J. Winiger, M. Eppenberger, D. Chelladurai, W. Heni, B. Baeuerle, U. Koch, P. Ma, C. Haffner, H. Xu, D. L. Elder, L. R. Dalton, J. Smajic, and J. Leuthold, “Broadband metallic fiber-to-chip couplers and a low-complexity integrated plasmonic platform,” *Nano Lett.* **21**, 4539–4545 (2021).
- ⁹²Y. Horst, T. Blatter, L. Kulmer, B. I. Bitachon, B. Baeuerle, M. Destraz, W. Heni, S. Koepfli, P. Habegger, M. Eppenberger, E. De Leo, C. Hoessbacher, D. L. Elder, S. R. Hammond, L. E. Johnson, L. R. Dalton, Y. Fedoryshyn, Y. Salamin, M. Burla, and J. Leuthold, “Transparent optical-THz-optical link at 240/192 Gbit/s over 5/115 m enabled by plasmonics,” *J. Lightwave Technol.* **40**, 1690–1697 (2022).
- ⁹³Q. Hu, R. Borkowski, Y. Lefevre, J. Cho, F. Buchali, R. Bonk, K. Schuh, E. De Leo, P. Habegger, M. Destraz, N. Del Medico, H. Duran, V. Tedaldi, C. Funck, Y. Fedoryshyn, J. Leuthold, W. Heni, B. Baeuerle, and C. Hoessbacher, “Ultrahigh-net-bitrate 363 Gbit/s PAM-8 and 279 Gbit/s polybinary optical transmission using plasmonic Mach-Zehnder modulator,” *J. Lightwave Technol.* **40**, 3338–3346 (2022).
- ⁹⁴P. Ma, Y. Salamin, A. Messner, B. Baeuerle, A. Emboras, W. Heni, A. Josten, F. Eltes, S. Abel, J. Fompeyrine, D. Elder, L. Dalton, J. Leuthold, B. B. Dingel, K. Tsukamoto, and S. Mikroulis, “Plasmonic modulators and photodetectors for communications,” in *Broadband Access Communication Technologies XV*, 2021.
- ⁹⁵W. Heni, Y. Fedoryshyn, B. Baeuerle, A. Josten, C. B. Hoessbacher, A. Messner, C. Haffner, T. Watanabe, Y. Salamin, U. Koch, D. L. Elder, L. R. Dalton, and J. Leuthold, “Plasmonic IQ modulators with attojoule per bit electrical energy consumption,” *Nat. Commun.* **10**, 1694 (2019).
- ⁹⁶S. Ummethala, T. Harter, K. Koehnle, Z. Li, S. Muehlbrandt, Y. Kutuvantavida, J. Kemal, P. Marin-Palomo, J. Schaefer, A. Tessmann, S. K. Garlapati, A. Bacher, L. Hahn, M. Walther, T. Zwick, S. Randel, W. Freude, and C. Koos, “THz-to-optical conversion in wireless communications using an ultra-broadband plasmonic modulator,” *Nat. Photonics* **13**, 519–524 (2019).
- ⁹⁷T. Blatter, Y. Horst, W. Heni, C. Pappas, A. Tsakyridis, G. Giamougiannis, M. Eppenberger, M. Kohl, U. Koch, M. Morales-Pegios, N. Pirois, and J. Leuthold, “Is there an ideal plasmonic modulator configuration,” in *European Conference on Optical Communications*, 2022.
- ⁹⁸J. Leuthold, Y. Horst, T. Blatter, L. Kulmer, L. Cherix, D. Moor, M. Eppenberger, M. Baumann, S. M. Koepfli, B. Baeuerle, W. Heni, C. Hoessbacher, E. d. Leo, Y. Fedoryshyn, U. Koch, M. Burla, and J. Smajic, “Plasmonics in future radio communications: Potential and challenges,” in *URSI AT-AP-RASC, Gran Canaria*, 2022.
- ⁹⁹P. Q. Liu, I. J. Luxmoore, S. A. Mikhailov, N. A. Savostianova, F. Valmorra, J. Faist, and G. R. Nash, “Highly tunable hybrid metamaterials employing splitting resonators strongly coupled to graphene surface plasmons,” *Nat. Commun.* **6**, 8969 (2015).
- ¹⁰⁰J. Zhang, Y. Kosugi, A. Otomo, Y. Nakano, and T. Tanemura, “Active metasurface modulator with electro-optic polymer using bimodal plasmonic resonance,” *Opt. Express* **25**, 30304 (2017).
- ¹⁰¹J. Zhang, Y. Kosugi, A. Otomo, Y.-L. Ho, J.-J. Delaunay, Y. Nakano, and T. Tanemura, “Electrical tuning of metal-insulator-metal metasurface with electro-optic polymer,” *Appl. Phys. Lett.* **113**, 231102 (2018).
- ¹⁰²A. Karvounis, V. V. Vogler-Neuling, F. U. Richter, E. Dénervaud, M. Timofeeva, and R. Grange, “Electro-optic metasurfaces based on barium titanate nanoparticle films,” *Adv. Opt. Mater.* **8**, 2000623 (2020).
- ¹⁰³F. Timpu, H. Weigand, F. Kaufmann, F. U. Richter, V.-V. Vogler-Neuling, A. Karvounis, R. Grange, R. Grange, M. F. Costa, and O. Frazao, “Towards active electro-optic lithium niobate metasurfaces,” *EPJ Web Conf.* **238**, 05003 (2020).

- ¹⁰⁴I.-C. Benea-Chelmus, M. L. Meretska, D. L. Elder, M. Tamagnone, L. R. Dalton, and F. Capasso, "Electro-optic spatial light modulator from an engineered organic layer," *Nat. Commun.* **12**, 5928 (2021).
- ¹⁰⁵X. Sun, H. Yu, N. Deng, D. Ban, G. Liu, and F. Qiu, "Electro-optic polymer and silicon nitride hybrid spatial light modulators based on a metasurface," *Opt. Express* **29**, 25543 (2021).
- ¹⁰⁶H. Weigand, V. V. Vogler-Neuling, M. R. Escalé, D. Pohl, F. U. Richter, A. Karvounis, F. Timpu, and R. Grange, "Enhanced electro-optic modulation in resonant metasurfaces of lithium niobate," *ACS Photonics* **8**, 3004–3009 (2021).
- ¹⁰⁷P. Berini, "Optical beam steering using tunable metasurfaces," *ACS Photonics* **9**, 2204–2218 (2022).
- ¹⁰⁸C. Damgaard-Carstensen, M. Thomaschewski, and S. I. Bozhevolnyi, "Electro-optic metasurface-based free-space modulators," *Nanoscale* **14**, 11407–11284 (2022).
- ¹⁰⁹A. Fedotova, L. Carletti, A. Zilli, F. Setzpfandt, I. Staude, A. Toma, M. Finazzi, C. De Angelis, T. Pertsch, D. N. Neshev, and M. Celebrano, "Lithium niobate meta-optics," *ACS Photonics* **9**, 3745–3763 (2022).
- ¹¹⁰T. Gu, H. J. Kim, C. Rivero-Baleine, and J. Hu, "Active metasurfaces: Lighting the path to commercial success," [arXiv:2205.12893](https://arxiv.org/abs/2205.12893) (2022).
- ¹¹¹Y. Ju, H. Zhou, Y. Zhao, F. Wang, Z. Yang, X. Deng, Z. Wu, D. Guoliang, and H. Zuo, "Hybrid resonance metasurface for a lithium niobate electro-optical modulator," *Opt. Lett.* **47**, 5905 (2022).
- ¹¹²E. Mikhcheeva, C. Kyrou, F. Bentata, S. Khadir, S. Cuffe, and P. Genevet, "Space and time modulations of light with metasurfaces: Recent progress and future prospects," *ACS Photonics* **9**, 1458–1482 (2022).
- ¹¹³X. Sun and F. Qiu, "Polarization independent high-speed spatial modulators based on an electro-optic polymer and silicon hybrid metasurface," *Photonics Res.* **10**, 2893 (2022).
- ¹¹⁴A. Weiss, C. Frydendahl, J. Bar-David, R. Zektzer, E. Edrei, J. Engelberg, N. Mazurski, B. Desiatov, and U. Levy, "Tunable metasurface using thin-film lithium niobate in the telecom regime," *ACS Photonics* **9**, 605–612 (2022).
- ¹¹⁵J. Zhang, J. Ma, M. Parry, M. Cai, R. Camacho-Morales, L. Xu, D. N. Neshev, and A. A. Sukhorukov, "Spatially entangled photon pairs from lithium niobate nonlocal metasurfaces," *Sci. Adv.* **8**, eabq4240 (2022).
- ¹¹⁶P. Steglich, C. Mai, C. Villringer, B. Dietzel, S. Bondarenko, V. Ksianzou, F. Villasmunta, C. Zesch, S. Pulver, M. Burger, J. Bauer, F. Heinrich, S. Schrader, F. Vitale, F. De Matteis, P. Proposito, M. Casalboni, and A. Mai, "Silicon-organic hybrid photonics: Overview of recent advances, electro-optical effects and CMOS-integration concepts," *J. Phys.: Photonics* **3**, 022009 (2021).
- ¹¹⁷C. Koos, S. He, and L. Vivien, "Silicon-organic hybrid (SOH) electro-optic modulators: Enhanced functionality for optical communications and THz signal processing," in *Smart Photonic and Optoelectronic Integrated Circuits 2022*, 2022.
- ¹¹⁸I. B. Khadka, N. R. Alluri, M. M. Alsdia, N. P. M. Joseph Raj, A. P. S. Prasanna, B. Ul Haq, S. J. Kim, and S.-H. Kim, "Ultra-low-power photodetector based on a high-photoresponse, plasmonic-effect-induced gateless quasi-freestanding graphene device," *Appl. Surf. Sci.* **610**, 155275 (2023).
- ¹¹⁹M. Furchi, A. Urich, A. Pospischil, G. Lilley, K. Unterrainer, H. Detz, P. Klang, A. M. Andrews, W. Schrenk, G. Strasser, and T. Mueller, "Microcavity-integrated graphene photodetector," *Nano Lett.* **12**, 2773–2777 (2012).
- ¹²⁰X. Gan, R.-J. Shiu, Y. Gao, I. Meric, T. F. Heinz, K. Shepard, J. Hone, S. Assefa, and D. Englund, "Chip-integrated ultrafast graphene photodetector with high responsivity," *Nat. Photonics* **7**, 883–887 (2013).
- ¹²¹K. Murali, N. Abraham, S. Das, S. Kallatt, and K. Majumdar, "Highly sensitive, fast graphene photodetector with responsivity $>10^6$ A/W using a floating quantum well gate," *ACS Appl. Mater. Interfaces* **11**, 30010–30018 (2019).
- ¹²²S. Schuler, J. E. Muench, A. Ruocco, O. Balci, D. v. Thourhout, V. Soriano, M. Romagnoli, K. Watanabe, T. Taniguchi, I. Goykhman, A. C. Ferrari, and T. Mueller, "High-responsivity graphene photodetectors integrated on silicon microring resonators," *Nat. Commun.* **12**, 3733 (2021).
- ¹²³V. Falcone, A. Ballabio, A. Barzaghi, C. Zucchetti, L. Anzi, F. Bottegoni, J. Frigerio, R. Sordan, P. Biagioni, and G. Isella, "Graphene/Ge microcrystal photodetectors with enhanced infrared responsivity," *APL Photonics* **7**, 046106 (2022).
- ¹²⁴S. M. Koepfli, M. Eppenberger, M. S.-B. Hossain, M. Baumann, M. Doderer, M. Destraz, P. Habegger, E. D. Leo, W. Heni, C. Hoessbacher, Y. Fedoryshyn, and J. Leuthold, ">500 GHz bandwidth graphene photodetector enabling highest-capacity plasmonic-to-plasmonic links," in *European Conference on Optical Communications*, 2022.
- ¹²⁵C. Delacour, S. Blaize, P. Grosse, J. M. Fedeli, A. Bruyant, R. Salas-Montiel, G. Lerondel, and A. Chelnokov, "Efficient directional coupling between silicon and copper plasmonic nanoslot waveguides: Toward metal-oxide-silicon nanophotonics," *Nano Lett.* **10**, 2922–2926 (2010).
- ¹²⁶D. Chelladurai, M. Doderer, U. Koch, Y. Fedoryshyn, C. Haffner, and J. Leuthold, "Low-loss hybrid plasmonic coupler," *Opt. Express* **27**, 11862 (2019).
- ¹²⁷P. Habegger, Y. Horst, S. Kopfli, E. D. Leo, D. Bisang, M. Destraz, V. Tedaldi, N. Meier, N. D. Medico, W. Wang, C. Hoessbacher, B. Baeuerle, W. Heni, and J. Leuthold, "Plasmonic 100-GHz electro-optic modulators for cryogenic applications," in *European Conference on Optical Communications*, 2022.
- ¹²⁸H. Xu *et al.*, "Ultra-high electro-optic coefficients, high index of refraction, and long-term stability from Diels-Alder cross-linkable binary molecular glasses," *Chem. Mater.* **32**, 1408–1421 (2020).
- ¹²⁹C. Hoessbacher, P. Habegger, M. Destraz, S. R. Hammond, L. E. Johnson, N. Meier, E. De Leo, B. Baeuerle, and W. Heni, "Plasmonic-organic-hybrid (POH) modulators—A powerful platform for next-generation integrated circuits," in *OSA Advanced Photonics Congress*, 2021, 2021.
- ¹³⁰C. M. Isborn, A. Leclercq, F. D. Vila, L. R. Dalton, J. L. Brédas, B. E. Eichinger, and B. H. Robinson, "Comparison of static first hyperpolarizabilities calculated with various quantum mechanical methods," *J. Phys. Chem. A* **111**, 1319–1327 (2007).
- ¹³¹M. G. Kuzyk, "Using fundamental principles to understand and optimize nonlinear-optical materials," *J. Mater. Chem.* **19**, 7444 (2009).
- ¹³²K. Y. Suponitsky, Y. Liao, and A. E. Masunov, "Electronic hyperpolarizabilities for donor-acceptor molecules with long conjugated bridges: Calculations versus experiment," *J. Phys. Chem. A* **113**, 10994–11001 (2009).
- ¹³³D. H. Bale, B. E. Eichinger, W. Liang, X. Li, L. R. Dalton, B. H. Robinson, and P. J. Reid, "Dielectric dependence of the first molecular hyperpolarizability for electro-optic chromophores," *J. Phys. Chem. B* **115**, 3505–3513 (2011).
- ¹³⁴L. R. Dalton, S. J. Benight, L. E. Johnson, D. B. Knorr, I. Kosilkin, B. E. Eichinger, B. H. Robinson, A. K.-Y. Jen, and R. M. Overney, "Systematic nanoengineering of soft matter organic electro-optic materials," *Chem. Mater.* **23**, 430–445 (2011).
- ¹³⁵M. G. Kuzyk, J. Pérez-Moreno, and S. Shafei, "Sum rules and scaling in nonlinear optics," *Phys. Rep.* **529**, 297–398 (2013).
- ¹³⁶K. Garrett, X. Sosa Vazquez, S. B. Egri, J. Wilmer, L. E. Johnson, B. H. Robinson, and C. M. Isborn, "Optimum exchange for calculation of excitation energies and hyperpolarizabilities of organic electro-optic chromophores," *J. Chem. Theory Comput.* **10**, 3821–3831 (2014).
- ¹³⁷L. E. Johnson, L. R. Dalton, and B. H. Robinson, "Optimizing calculations of electronic excitations and relative hyperpolarizabilities of electrooptic chromophores," *Acc. Chem. Res.* **47**, 3258–3265 (2014).
- ¹³⁸A. A. Kocherzhenko, X. A. Sosa Vazquez, J. M. Milanese, and C. M. Isborn, "Absorption spectra for disordered aggregates of chromophores using the exciton model," *J. Chem. Theory Comput.* **13**, 3787–3801 (2017).
- ¹³⁹D. L. Elder, L. E. Johnson, A. F. Tillack, B. H. Robinson, W. Heni, C. B. Hoessbacher, Y. Fedoryshyn, Y. Salamin, B. Baeuerle, A. Josten, M. Ayata, U. Koch, J. Leuthold, C. Haffner, and L. R. Dalton, "Multi-scale theory-assisted nano-engineering of plasmonic-organic hybrid electro-optic device performance," in *SPIE OPTO, San Francisco, CA*, edited by Y. Koike, T. Kaino, F. Kajzar, and C. E. Tabor (SPIE, 2018), p. 105290K.
- ¹⁴⁰A. A. Kocherzhenko, S. V. Shedje, X. Sosa Vazquez, J. Maat, J. Wilmer, A. F. Tillack, L. E. Johnson, and C. M. Isborn, "Unraveling excitonic effects for the first hyperpolarizabilities of chromophore aggregates," *J. Phys. Chem. C* **123**, 13818–13836 (2019).
- ¹⁴¹J. R. Hammond and K. Kowalski, "Parallel computation of coupled-cluster hyperpolarizabilities," *J. Chem. Phys.* **130**, 194108 (2009).
- ¹⁴²L. E. Johnson, M. T. Casford, D. L. Elder, P. B. Davies, M. S. Johal, and N. Kobayashi, *SFG Characterization of a Cationic ONLO Dye in Biological Thin Films*, edited by F. Ouchen and I. Rau (2013), Vol. 8817, p. 88170P.
- ¹⁴³S. R. Marder, D. N. Beratan, and L.-T. Cheng, "Approaches for optimizing the first electronic hyperpolarizability of conjugated organic molecules," *Science* **252**, 103–106 (1991).

- ¹⁴⁴A. F. Tillack, L. E. Johnson, D. L. Elder, A. A. Kocherzhenko, C. M. Isborn, L. R. Dalton, and B. H. Robinson, "Poling-induced birefringence in OEO materials under nanoscale confinement," in *Organic and Hybrid Sensors and Bioelectronics*, XI 2018.
- ¹⁴⁵S. J. Benight, D. B. Knorr, L. E. Johnson, P. A. Sullivan, D. Lao, J. Sun, L. S. Kocherlakota, A. Elangovan, B. H. Robinson, R. M. Overney, and L. R. Dalton, "Nano-engineering lattice dimensionality for a soft matter organic functional material," *Adv. Mater.* **24**, 3263–3268 (2012).
- ¹⁴⁶A. R. Leach, *Molecular Modeling: Principles and Applications*, 2nd ed. (Pearson Education, Harlow, 2001).
- ¹⁴⁷M. R. Leahy-Hoppa, P. D. Cunningham, J. A. French, and L. M. Hayden, "Atomistic molecular modeling of the effect of chromophore concentration on the electro-optic coefficient in nonlinear optical polymers," *J. Phys. Chem. A* **110**, 5792–5797 (2006).
- ¹⁴⁸A. F. Tillack, "Electro-optic material design criteria derived from condensed matter simulations using the level-of-detail coarse-graining approach," Ph.D. dissertation, University of Washington, Seattle, WA, 2015.
- ¹⁴⁹B. Merrifield, "Solid phase synthesis," *Science* **232**, 341–347 (1986).
- ¹⁵⁰C. D. Bain and G. M. Whitesides, "Molecular-level control over surface order in self-assembled monolayer films of thiols on gold," *Science* **240**, 62–63 (1988).
- ¹⁵¹H. E. Katz, G. Scheller, T. M. Putvinski, M. L. Schilling, W. L. Wilson, and C. E. D. Chidsey, "Polar orientation of dyes in robust multilayers by zirconium phosphate-phosphonate Interlayers," *Science* **254**, 1485–1487 (1991).
- ¹⁵²L. H. Dubois and R. G. Nuzzo, "Synthesis, structure, and properties of model organic surfaces," *Annu. Rev. Phys. Chem.* **43**, 437–463 (1992).
- ¹⁵³T. J. Marks and M. A. Ratner, "Design, synthesis, and properties of molecule-based assemblies with large second-order optical nonlinearities," *Angew. Chem., Int. Ed. Engl.* **34**, 155–173 (1995).
- ¹⁵⁴W. Lin, W. Lin, G. K. Wong, and T. J. Marks, "Supramolecular approaches to second-order nonlinear optical materials. Self-assembly and microstructural characterization of Intrinsically acentric [(Aminophenyl)azo]pyridinium superlattices," *J. Am. Chem. Soc.* **118**, 8034–8042 (1996).
- ¹⁵⁵S. Yitzchaik and T. J. Marks, "Chromophoric self-assembled superlattices," *Acc. Chem. Res.* **29**, 197–202 (1996).
- ¹⁵⁶G. Decher, "Fuzzy nanoassemblies: Toward layered polymeric multicomposites," *Science* **277**, 1232–1237 (1997).
- ¹⁵⁷L. E. Canne, P. Botti, R. J. Simon, Y. Chen, E. A. Dennis, and S. B. H. Kent, "Chemical protein synthesis by solid phase ligation of unprotected peptide segments," *J. Am. Chem. Soc.* **121**, 8720–8727 (1999).
- ¹⁵⁸H. C. Kolb, M. G. Finn, and K. B. Sharpless, "Click chemistry: Diverse chemical function from a few good reactions," *Angew. Chem., Int. Ed.* **40**, 2004–2021 (2001).
- ¹⁵⁹H. E. Katz, W. L. Wilson, and G. Scheller, "Chromophore structure, second harmonic generation, and orientational order in zirconium phosphate-phosphate self-assembled multilayers," *J. Am. Chem. Soc.* **116**, 6636–6640 (2002).
- ¹⁶⁰A. Kumar, N. L. Abbott, H. A. Biebuyck, E. Kim, and G. M. Whitesides, "Patterned self-assembled monolayers and meso-scale phenomena," *Acc. Chem. Res.* **28**, 219–226 (2002).
- ¹⁶¹M. E. van der Boom, G. Evmenenko, J. E. Malinsky, W. Lin, P. Dutta, T. J. Marks, and T. J. Marks, "Nanoscale consecutive self-assembly of thin-film molecular materials for electrooptic switching. Chemical streamlining and ultrahigh response chromophores," *Langmuir* **18**, 3704–3707 (2002).
- ¹⁶²P. Zhu, M. E. van der Boom, H. Kang, G. Evmenenko, P. Dutta, and T. J. Marks, "Realization of expeditious layer-by-layer siloxane-based self-assembly as an efficient route to structurally regular acentric superlattices with large electro-optic responses," *Chem. Mater.* **14**, 4982–4989 (2002).
- ¹⁶³A. Facchetti, A. Abbotto, L. Beverina, M. E. van der Boom, P. Dutta, G. Evmenenko, G. A. Pagani, and T. J. Marks, "Layer-by-layer self-assembled pyrrole-based donor-acceptor chromophores as electro-optic materials," *Chem. Mater.* **15**, 1064–1072 (2003).
- ¹⁶⁴S. M. George, "Atomic layer deposition: An overview," *Chem. Rev.* **110**, 111–131 (2009).
- ¹⁶⁵S. M. George, B. Yoon, and A. A. Dameron, "Surface chemistry for molecular layer deposition of organic and hybrid organic-inorganic polymers," *Acc. Chem. Res.* **42**, 498–508 (2009).
- ¹⁶⁶O. Acton, D. Hutchins, L. Árnadóttir, T. Weidner, N. Cernetic, G. G. Ting, T.-W. Kim, D. G. Castner, H. Ma, and A. K.-Y. Jen, "Spin-cast and patterned organophosphate self-assembled monolayer dielectrics on metal-oxide-activated Si," *Adv. Mater.* **23**, 1899–1902 (2011).
- ¹⁶⁷P. T. Hammond, "Engineering materials layer-by-layer: Challenges and opportunities in multilayer assembly," *AIChE J.* **57**, 2928–2940 (2011).
- ¹⁶⁸K. Everaerts, J. D. Emery, D. Jariwala, H. J. Karmel, V. K. Sangwan, P. L. Prabhurashi, M. L. Geier, J. J. McMorro, M. J. Bedzyk, A. Facchetti, M. C. Hersam, and T. J. Marks, "Ambient-processable high capacitance Hafnia-organic self-assembled nanodielectrics," *J. Am. Chem. Soc.* **135**, 8926–8939 (2013).
- ¹⁶⁹Y.-G. Ha, K. Everaerts, M. C. Hersam, and T. J. Marks, "Hybrid gate dielectric materials for unconventional electronic circuitry," *Acc. Chem. Res.* **47**, 1019–1028 (2014).
- ¹⁷⁰X. Meng, "An overview of molecular layer deposition for organic and organic-inorganic hybrid materials: Mechanisms, growth characteristics, and promising applications," *J. Mater. Chem. A* **5**, 18326–18378 (2017).
- ¹⁷¹M. Singh, N. Kaur, and E. Comini, "The role of self-assembled monolayers in electronic devices," *J. Mater. Chem. C* **8**, 3938–3955 (2020).
- ¹⁷²N. G. Caculitan, P. H. Scudder, A. Rodriguez, J. L. Casson, H.-L. Wang, J. M. Robinson, and M. S. Johal, "In situ kinetics of layer-by-layer assembled nonlinear-optical-active amphiphiles from dynamic surface force measurements," *Langmuir* **20**, 8735–8739 (2004).
- ¹⁷³C. Queffelec, M. Petit, P. Janvier, D. A. Knight, and B. Bujoli, "Surface modification using phosphonic acids and esters," *Chem. Rev.* **112**, 3777–3807 (2012).
- ¹⁷⁴N. K. Devaraj and M. G. Finn, "Introduction: Click chemistry," *Chem. Rev.* **121**, 6697–6698 (2021).
- ¹⁷⁵W. Jin, P. V. Johnston, D. L. Elder, A. F. Tillack, B. C. Olbricht, J. Song, P. J. Reid, R. Xu, B. H. Robinson, and L. R. Dalton, "Benzocyclobutene barrier layer for suppressing conductance in nonlinear optical devices during electric field poling," *Appl. Phys. Lett.* **104**, 243304 (2014).
- ¹⁷⁶Y. Liao, S. Bhattacharjee, K. A. Firestone, B. E. Eichinger, R. Paranj, C. A. Anderson, B. H. Robinson, P. J. Reid, and L. R. Dalton, "Antiparallel-aligned neutral-ground-state and zwitterionic chromophores as a nonlinear optical material," *J. Am. Chem. Soc.* **128**, 6847–6853 (2006).
- ¹⁷⁷M. Halter, Y. Liao, R. M. Plocinik, D. C. Coffey, S. Bhattacharjee, U. Mazur, G. J. Simpson, B. H. Robinson, and S. L. Keller, "Molecular self-assembly of mixed high-beta zwitterionic and neutral ground-state NLO chromophores," *Chem. Mater.* **20**, 1778–1787 (2008).
- ¹⁷⁸Y. Shi, C. Zhang, H. Zhang, J. H. Bechtel, L. R. Dalton, B. H. Robinson, and W. H. Steier, "Low (Sub-1-Volt) Halfwave voltage polymeric electro-optic modulators achieved by controlling chromophore shape," *Science* **288**, 119–122 (2000).
- ¹⁷⁹D. L. Elder, C. Haffner, W. Heni, Y. Fedoryshyn, K. E. Garrett, L. E. Johnson, R. A. Campbell, J. D. Avila, B. H. Robinson, J. Leuthold, and L. R. Dalton, "Effect of rigid bridge-protection units, quadrupolar interactions, and blending in organic electro-optic chromophores," *Chem. Mater.* **29**, 6457–6471 (2017).
- ¹⁸⁰W. Jin, P. V. Johnston, D. L. Elder, K. T. Manner, K. E. Garrett, W. Kaminsky, R. Xu, B. H. Robinson, and L. R. Dalton, "Structure-function relationship exploration for enhanced thermal stability and electro-optic activity in monolithic organic NLO chromophores," *J. Mater. Chem. C* **4**, 3119–3124 (2016).
- ¹⁸¹M. Y. Abdelatty, A. O. Zaki, and M. A. Swillam, "Hybrid silicon plasmonic organic directional coupler-based modulator," *Appl. Phys. A* **123**, 11 (2016).
- ¹⁸²Y. Tominari, T. Yamada, T. Kaji, C. Yamada, and A. Otomo, "Photostability of organic electro-optic polymer under practical high intensity continuous-wave 1550 nm laser irradiation," *Jpn. J. Appl. Phys.* **60**, 101002 (2021).
- ¹⁸³F. Ullah, N. Deng, and F. Qiu, "Recent progress in electro-optic polymer for ultra-fast communication," *Photonix* **2**, 13 (2021).
- ¹⁸⁴S. Kamada, R. Ueda, C. Yamada, K. Tanaka, T. Yamada, and A. Otomo, "Superiorly low half-wave voltage electro-optic polymer modulator for visible photonics," *Opt. Express* **30**, 19771 (2022).
- ¹⁸⁵Y. Tominari, T. Yamada, T. Kaji, and A. Otomo, "Photochemical stability of organic electro-optic polymer at 1310-nm wavelength," *IEICE Trans. Electron.* (published online, 2022).

- ¹⁸⁶Q. Zeng, X. Chen, A. Rahman, Z. Zeng, Z. Liang, L. Shi, Z. Huang, S. Bo, F. Liu, and J. Wang, "A modifiable double donor based on bis(*N*-ethyl-*N*-hydroxyethyl)aniline for organic optical nonlinear chromophores," *Mater. Chem. Front.* **6**, 1079–1090 (2022).
- ¹⁸⁷Z. Zeng, J. Liu, T. Luo, Z. Li, J. Liao, W. Zhang, L. Zhang, and F. Liu, "Electro-optic crosslinkable chromophores with ultrahigh electro-optic coefficients and long-term stability," *Chem. Sci.* **13**, 13393–13402 (2022).
- ¹⁸⁸H. Zhang, S. Bo, J. Zhang, Y. Ao, and M. Li, "Synthesis of new type of nonlinear optical chromophores: The introduction of a novel aromatic amine donor 1-oxajulolidine to enhance the electro-optical activity of organic second-order nonlinear optical materials," *Dyes Pigm.* **209**, 110891 (2023).
- ¹⁸⁹B. Huang, Z. Zhang, M. Li, K. Zhang, T. Liu, H. Jiang, Q. Wang, and J. Xing, "Simulation of hybrid silicon nitride/polymer Mach-Zehnder optical modulator beyond 170 GHz," *Front. Phys.* **10**, 1079167 (2022).
- ¹⁹⁰F. Qiu, A. M. Spring, D. Maeda, M.-a. Ozawa, K. Odoi, A. Otomo, I. Aoki, and S. Yokoyama, "A hybrid electro-optic polymer and TiO₂ double-slot waveguide modulator," *Sci. Rep.* **5**, 8561 (2015).
- ¹⁹¹T. Rutirawut, W. Talataisong, and F. Y. Gardes, "Designs of silicon nitride slot waveguide modulators with electro-optic polymer and the effect of induced charges in Si-substrate on their performance," *IEEE Photonics J.* **13**, 6600715 (2021).
- ¹⁹²S. R. Hammond, K. M. O'Malley, H. Xu, D. L. Elder, and L. E. Johnson, "Organic electro-optic materials combining extraordinary nonlinearity with exceptional stability to enable commercial applications," in *Proceedings of SPIE*, edited by I. Rau, O. Sugihara, and W. M. Shensky (SPIE, 2022).
- ¹⁹³C. Ye, S. Khan, Z. R. Li, E. Simsek, and V. J. Sorger, "λ-Size ITO and graphene-based electro-optic modulators on SOI," *IEEE J. Sel. Top. Quantum Electron.* **20**, 40–49 (2014).
- ¹⁹⁴Z. Ma, Z. Li, K. Liu, C. Ye, and V. J. Sorger, "Indium-tin-oxide for high-performance electro-optic modulation," *Nanophotonics* **4**, 198–213 (2015).
- ¹⁹⁵R. Amin, R. Maiti, Y. Gui, C. Suer, M. Miscuglio, E. Heidari, R. T. Chen, H. Dalir, and V. J. Sorger, "GHz plasmonic broadband ITO MZI modulator in Si photonics," in *OSA Advanced Photonics Congress 2021*, 2021.
- ¹⁹⁶R. Amin, R. Maiti, Y. Gui, C. Suer, M. Miscuglio, E. Heidari, J. B. Khurgin, R. T. Chen, H. Dalir, and V. J. Sorger, "Heterogeneously integrated ITO plasmonic Mach-Zehnder interferometric modulator on SOI," *Sci. Rep.* **11**, 1287 (2021).
- ¹⁹⁷K. Q. Le, "ITO-based electro-optical modulator integrated in silicon-on-insulator waveguide using surface plasmon interference," *Phys. B* **602**, 412313 (2021).
- ¹⁹⁸E. S. Lotkov, A. S. Baburin, I. A. Ryzhikov, O. S. Sorokina, A. I. Ivanov, A. V. Zverev, V. V. Ryzhkov, I. V. Bykov, A. V. Baryshev, Y. V. Panfilov, and I. A. Rodionov, "ITO film stack engineering for low-loss silicon optical modulators," *Sci. Rep.* **12**, 6321 (2022).
- ¹⁹⁹J. D. Morse, K. G. McCammon, C. F. McConaghy, D. A. Masquelier, H. E. Garrett, M. E. Lowry, and M. E. Lowry, "Characterization of lithium niobate electro-optic modulators at cryogenic temperatures," *Proc. SPIE* **2150**, 283–291 (1994).
- ²⁰⁰F. Eltes, G. E. Villarreal-Garcia, D. Caimi, H. Siegwart, A. A. Gentile, A. Hart, P. Stark, G. D. Marshall, M. G. Thompson, J. Barreto, J. Fompeyrine, and S. Abel, "An integrated optical modulator operating at cryogenic temperatures," *Nat. Mater.* **19**, 1164 (2020).
- ²⁰¹J. D. Witmer, T. P. McKenna, P. Arrangoiz-Arriola, R. Van Laer, E. Alex Wol-lack, F. Lin, A. K.-Y. Jen, J. Luo, and A. H. Safavi-Naeini, "A silicon-organic hybrid platform for quantum microwave-to-optical transduction," *Quantum Sci. Technol.* **5**, 034004 (2020).
- ²⁰²F. Lecocq, F. Quinlan, K. Cicak, J. Aumentado, S. A. Diddams, and J. D. Teufel, "Control and readout of a superconducting qubit using a photonic link," *Nature* **591**, 575–579 (2021).
- ²⁰³A. Youssefi, I. Shomroni, Y. J. Joshi, N. R. Bernier, A. Lukashchuk, P. Uhrich, L. Qiu, and T. J. Kippenberg, "A cryogenic electro-optic interconnect for superconducting devices," *Nat. Electron.* **4**, 326–332 (2021).
- ²⁰⁴M. Cherchi, E. Mykkanen, A. Kemppinen, K. Tappura, J. Govenius, M. Prunnila, G. Delrosso, T. Hakkarainen, J. Viherlala, M. Castanedo, M. Bieber, S. Steinhauer, V. Zwiller, S. M. Koepfli, J. Leuthold, and E. De Leo, "A path towards attojoule cryogenic communication," in European Conference on Optical Communications, (2022).
- ²⁰⁵R. D. Delaney, M. D. Urmey, S. Mittal, B. M. Brubaker, J. M. Kindem, P. S. Burns, C. A. Regal, and K. W. Lehnert, "Superconducting-qubit readout via low-backaction electro-optic transduction," *Nature* **606**, 489–493 (2022).
- ²⁰⁶P. Pintus, A. Singh, W. Xie, L. Ranzani, M. V. Gustafsson, M. A. Tran, C. Xiang, J. Peters, J. E. Bowers, and M. Soltani, "Ultralow voltage, high-speed, and energy-efficient cryogenic electro-optic modulator," *Optica* **9**, 1176 (2022).
- ²⁰⁷A. Schwarzenberger, A. Kuzmin, C. Eschenbaum, C. Fullner, A. Mertens, L. E. Johnson, D. L. Elder, S. R. Hammond, L. Dalton, S. Randel, W. Freude, and C. Koos, "Cryogenic operation of a silicon-organic hybrid (SOH) modulator at 50 Gbit/s and 4K ambient temperature," in European Conference on Optical Communications, 2022.
- ²⁰⁸X.-B. Xu, W.-T. Wang, L.-Y. Sun, and C.-L. Zou, "Hybrid superconducting photonic-phononic chip for quantum information processing," *Chip* **1**, 100016 (2022).
- ²⁰⁹S. Verghese, "Self-driving cars and lidar," in Conference on Lasers and Electro-Optics, 2017.
- ²¹⁰T. Fahey, H. Pham, A. Gardi, R. Sabatini, D. Stefanelli, I. Goodwin, and D. W. Lamb, "Active and passive electro-optical sensors for Health assessment in food crops," *Sensors* **21**, 171 (2020).
- ²¹¹K. W. Hudnut, B. A. Brooks, K. Scharer, J. L. Hernandez, T. E. Dawson, M. E. Oskin, J. Ramon Arrowsmith, C. A. Goulet, K. Blake, M. L. Boggs, S. Bork, C. L. Glennie, J. C. Fernandez-Diaz, A. Singhanian, D. Hauser, and S. Sorhus, "Airborne lidar and electro-optical imagery along surface ruptures of the 2019 ridgecrest earthquake sequence, Southern California," *Seismol. Res. Lett.* **91**, 2096–2107 (2020).
- ²¹²J. E. Bowers, L. Chang, M. Li, Q. Lin, W. Xie, X. Wang, H. Shu, and K. Vahala, "Silicon photonic integrated circuits for LiDAR," in *2022 IEEE Photonics Conference (IPC)* (IEEE, 2022), pp. 1–3.
- ²¹³T. A. Morris, J. M. Wheeler, M. J. Grant, M. J. Digonnet, K. Kalli, G. Bram-billa, and S. O. O'Keeffe, "Advances in optical gyroscopes," in Seventh European Workshop on Optical Fibre Sensors, 2019.
- ²¹⁴M. A. Nahmias, T. F. de Lima, A. N. Tait, H.-T. Peng, B. J. Shastri, and P. R. Prucnal, "Photonic multiply-accumulate operations for neural networks," *IEEE J. Sel. Top. Quantum Electron.* **26**, 1–18 (2020).
- ²¹⁵N. Peserico, X. Ma, B. Shastri, V. J. Sorger, G. Volpe, J. B. Pereira, D. Brunner, and A. Ozcan, "Photonic tensor core for machine learning: A review," in *Emerging Topics in Artificial Intelligence (ETAI)* (SPIE, 2022), p. 2022.
- ²¹⁶C. Wang, M. Zhang, B. Stern, M. Lipson, and M. Lončar, "Nanophotonic lithium niobate electro-optic modulators," *Opt. Express* **26**, 1547 (2018).
- ²¹⁷M. Zhang, C. Wang, P. Kharel, D. Zhu, and M. Lončar, "Integrated lithium niobate electro-optic modulators: When performance meets scalability," *Optica* **8**, 652 (2021).
- ²¹⁸E. Berikaa, M. S. Alam, and D. V. Plant, "Net 400-Gbps/λ IMDD transmission using a single-DAC DSP-free transmitter and a thin-film lithium niobate MZM," *Opt. Lett.* **47**, 6273 (2022).
- ²¹⁹M. Wang, Z. Fang, J. Lin, R. Wu, J. Chen, Z. Liu, H. Zhang, L. Qiao, and Y. Cheng, "Integrated active lithium niobate photonic devices," *Jpn. J. Appl. Phys.* **62**, SC0801 (2023).
- ²²⁰E. Berikaa, M. S. Alam, and D. V. Plant, "Beyond 300 Gbps short-reach links using TFLN MZMs with 500 mV_{pp} and linear equalization," *IEEE Photonics Technol. Lett.* **35**, 140–143 (2023).
- ²²¹C. Wang, M. Zhang, X. Chen, M. Bertrand, A. Shams-Ansari, S. Chandrasekhar, P. Winzer, and M. Lončar, "Integrated lithium niobate electro-optic modulators operating at CMOS-compatible voltages," *Nature* **562**, 101–104 (2018).
- ²²²S. Abel, F. Eltes, J. E. Ortman, A. Messner, P. Castera, T. Wagner, D. Urbonas, A. Rosa, A. M. Gutierrez, D. Tulli, P. Ma, B. Baeuerle, A. Josten, W. Heni,

- D. Caimi, L. Czornomaz, A. A. Demkov, J. Leuthold, P. Sanchis, and J. Fompeyrine, "Large Pockels effect in micro- and nanostructured barium titanate integrated on silicon," *Nat. Mater.* **18**, 42–47 (2018).
- ²²³A. Melikyan, N. Lindenmann, S. Walheim, P. M. Leufke, S. Ulrich, J. Ye, P. Vincze, H. Hahn, T. Schimmel, C. Koos, W. Freude, and J. Leuthold, "Surface plasmon polariton absorption modulator," *Opt. Express* **19**, 8855 (2011).
- ²²⁴A. Rahim, A. Hermans, B. Wohlfeil, D. Petousi, B. Kuyken, D. Van Thourhout, and R. Baets, "Taking silicon photonics modulators to a higher performance level: State-of-the-art and a review of new technologies," *Adv. Photonics* **3**, 3 (2021).
- ²²⁵R. Amin, J. B. Khurgin, and V. J. Sorger, "Waveguide-based electro-absorption modulator performance: Comparative analysis," *Opt. Express* **26**, 15445 (2018).
- ²²⁶L. Mastronardi, M. Banakar, A. Z. Khokhar, N. Hattasan, T. Rutirawut, T. D. Bucio, K. M. Grabska, C. Littlejohns, A. Bazin, G. Mashanovich, and F. Y. Gardes, "High-speed Si/GeSi hetero-structure electro absorption modulator," *Opt. Express* **26**, 6663 (2018).
- ²²⁷Z. Liu, X. Li, C. Niu, J. Zheng, C. Xue, Y. Zuo, and B. Cheng, "56 Gbps high-speed Ge electro-absorption modulator," *Photonics Res.* **8**, 1648 (2020).
- ²²⁸A. Chen and E. J. Murphy, *Broadband Optical Modulators* (CRC Press, Boca Raton, FL, 2012).
- ²²⁹J. Capmany and P. Munoz, "Integrated microwave photonics for radio access networks," *J. Lightwave Technol.* **32**, 2849–2861 (2014).
- ²³⁰A. Tuniz, "Nanoscale nonlinear plasmonics in photonic waveguides and circuits," *La Rivista del Nuovo Cimento* **44**, 193–249 (2021).
- ²³¹G. Sinatkas, T. Christopoulos, O. Tsilipakos, and E. E. Kriezis, "Electro-optic modulation in integrated photonics," *J. Appl. Phys.* **130**, 010901 (2021).
- ²³²R. Amin, R. Maiti, Y. Gui, C. Suer, M. Miscuglio, E. Heidari, R. T. Chen, H. Dalir, and V. J. Sorger, "Sub-wavelength GHz-fast broadband ITO Mach-Zehnder modulator on silicon photonics," *Optica* **7**, 333 (2020).
- ²³³P. Kaur, A. Boes, G. Ren, T. G. Nguyen, G. Roelkens, and A. Mitchell, "Hybrid and heterogeneous photonic integration," *APL Photonics* **6**, 061102 (2021).
- ²³⁴C. A. Thraskias, E. N. Lallas, N. Neumann, L. Schares, B. J. Offrein, R. Henker, D. Plettemeier, F. Ellinger, J. Leuthold, and I. Tomkos, "Survey of photonic and plasmonic interconnect technologies for intra-datacenter and high-performance computing communications," *IEEE Commun. Surv. Tutorials* **20**, 2758–2783 (2018).
- ²³⁵J. Witzens, "High-speed silicon photonics modulators," *Proc. IEEE* **106**, 2158–2182 (2018).
- ²³⁶E. Berikaa, M. Samiul Alam, and D. V. Plant, "Silicon photonic modulators for net 300 Gbps/λ IM/DD and Net 1 Tbps/λ coherent transmission using all-electronic equalization," *Opt. Fiber Technol.* **74**, 103056 (2022).
- ²³⁷U. Koch, C. Uhl, H. Hettrich, Y. Fedoryshyn, D. Moor, M. Baumann, C. Hoessbacher, W. Heni, B. Baeuerle, B. I. Bitachon, A. Josten, M. Ayata, H. Xu, D. L. Elder, L. R. Dalton, E. Mentovich, P. Bakopoulos, S. Lischke, A. Krüger, L. Zimmermann, D. Tsiokos, N. Pleros, M. Möller, and J. Leuthold, "Plasmonics—High-speed photonics for co-integration with electronics," *Jpn. J. Appl. Phys.* **60**, SB0806 (2021).
- ²³⁸D. Moor, Y. Fedoryshyn, H. Langenhagen, J. Müllrich, R. Schmid, C. Uhl, M. Möller, U. Koch, Y. Horst, B. I. Bitachon, W. Heni, B. Baeuerle, M. Destraz, H. Xu, L. E. Delwin, L. E. Johnson, P. Bakopoulos, E. Mentovich, L. Zimmermann, and J. Leuthold, "180 Gbd electronic-plasmonic IC transmitter," in Optical Fiber Communication Conference (OFC), 2022, 2022.